Published in final edited form as:
Biochim Biophys Acta. 2012 May ; 1822(5): 794–814. doi:10.1016/j.bbadis.2011.12.002.

Manganese superoxide dismutase, MnSOD and its mimics

Sumitra Miriyala[1], **Ivan Spasojevic**[2], **Artak Tovmasyan**[3], **Daniela Salvemini**[4], **Zeljko Vujaskovic**[3], **Daret St. Clair**[1,*], and **Ines Batinic-Haberle**[3,*]

[1]Graduate Center for Toxicology, University of Kentucky, Lexington, KY, 40536

[2]Department of Medicine, Duke University Medical Center, Durham, NC 27710

[3]Department of Radiation Oncology, Duke University Medical Center, Durham, NC 27710

[4]Department of Pharmacological and Physiological Science, Saint Louis University School of Medicine, 1402 South Grand Blvd, St. Louis, MO 63104

Abstract

Increased understanding of the role of mitochondria under physiological and pathological conditions parallels increased exploration of synthetic and natural compounds able to mimic MnSOD – endogenous mitochondrial antioxidant defense essential for the existence of virtually all aerobic organisms from bacteria to humans. This review describes most successful mitochondrially-targeted redox-active compounds, Mn porphyrins and $MitoQ_{10}$ in detail, and briefly addresses several other compounds that are either catalysts of $O_2^{\cdot-}$ dismutation, or its non-catalytic scavengers, and that reportedly attenuate mitochondrial dysfunction. While not a true catalyst (SOD mimic) of $O_2^{\cdot-}$ dismutation, $MitoQ_{10}$ oxidizes $O_2^{\cdot-}$ to O_2 with a high rate constant. *In vivo* it is readily reduced to quinol, $MitoQH_2$, which in turn reduces $ONOO^-$ to $^{\cdot}NO_2$, producing semiquinone radical that subsequently dismutes to $MitoQ_{10}$ and $MitoQH_2$, completing the "catalytic" cycle. In $MitoQ_{10}$, the redox-active unit was coupled to alkyl chain and monocationic triphenylphosphonium ion in order to reach mitochondria. Mn porphyrin-based SOD mimics, however, were designed so that their multiple cationic charge and alkyl chains determine both their remarkable SOD potency and carry them into mitochondria. Several animal efficacy studies such as skin carcinogenesis and UVB-mediated mtDNA damage, and subcellular distribution studies of *Saccharomyces cerevisiae* and mouse heart provided unambiguous evidence that Mn porphyrins mimic the site and action of MnSOD, which in turn contributes to their efficacy in numerous *in vitro* and *in vivo* models of oxidative stress. Within a class of Mn porphyrins, lipophilic analogues are particularly effective for treating central nervous system injuries where mitochondria play key role.

Introduction

Superoxide ($O_2^{\cdot-}$) has a prominent role in oxidative stress and impacts the production of a plethora of other reactive species, such as H_2O_2, peroxynitrite ($ONOO^-$), peroxynitrite

*Corresponding authors Daret St. Clair, Ph.D., Professor of Toxicology, James Graham Brown Foundation Endowed Chair in Neurosciences, 454 HSRB, Graduate Center for Toxicology, University of Kentucky, Lexington, KY 40536, Tel: 859-257-3956., dstcl00@.uky.edu. Ines Batinic-Haberle, Ph. D., Associate Professor, Department of Radiation Oncology-Cancer Biology, Duke University Medical Center, Durham, NC 27710, Tel: 919-684-2101, Fax: 919-684-8718, ibatinic@duke.edu.

degradation products ($^{\cdot}OH$, $^{\cdot}NO_2$, $CO_3^{\cdot-}$), lipid peroxyl ($RO_2^{\cdot}$) and alkoxyl ($RO^{\cdot}$) radicals. Its one-electron reduction product, H_2O_2, is a dominant signaling molecule [1]. Endogenous antioxidants maintain reactive species at nanomolar levels, and any increase results in redox imbalance (oxidative stress) [2], which in turn leads to excessive inflammatory and immune responses. The superoxide dismutase family of enzymes is comprised of MnSOD located in the mitochondrial matrix, and Cu, ZnSOD located in the mitochondrial intermembrane space, cytosol and extracellular space. These key enzymes catalyze the dismutation (disproportionation) of superoxide anion radical to hydrogen peroxide and molecular oxygen [2]. In doing so, they protect cells against oxidative damage and regulate the cellular concentration of $O_2^{\cdot-}$ and its reactive progeny under both physiological and pathological conditions [2]. Mutations in Cu, ZnSOD have been linked to amyotrophic lateral sclerosis, and deficiency of Cu, ZnSOD has been associated with accelerated aging and a higher incidence of cancer [3–6]. However, aerobic life without MnSOD is not sustainable. A substantial body of evidence has been established by Fridovich and his associates [7, 8] that MnSOD is ubiquitous metalloenzyme essential for the survival of all aerobic organisms from bacteria to humans. It is even found in many anaerobes where it protects the cell during exposure to aerobic conditions [9]. Cambialistic enzymes are found in several anaerobic bacteria, such as *Propionibacterium shermanii*, and have either Mn^{3+} or Fe^{3+} at their active site. When growing anaerobically, these enzymes contain Fe^{3+}, but when grown under micro aerobic conditions, these enzymes have Mn^{3+} at their active site [10]. MnSOD is encoded by a nuclear gene and is transported across two mitochondrial membranes to the matrix. In humans, this translocation involves translation of a proenzyme which includes a 24-amino acid N-terminal peptide targeting the protein to the mitochondria. In mice, the lack of MnSOD, or the complete elimination of its expression, causes dilated cardiomyopathy and neurodegeneration leading to early postnatal death. These mice exhibit severe oxidative damage to mitochondria and are also extremely sensitive to hyperoxia [11, 12]. It has been clearly demonstrated that heterozygous MnSOD knock-out mice have a 50% decrease in MnSOD enzyme activity in all tissues compared to wild-type mice, resulting in an age-dependent increase in oxidative DNA damage (8-hydroxy-2′-deoxyguanosine) in both nucleus and mitochondria.

A critical role of MnSOD under physiological and pathological conditions has recently been reviewed in details by St. Clair group [13, 14]. Herein, we briefly summarized the role of MnSOD in general, and tumorigenesis in particular. The MnSOD enzyme is involved in maintaining nanomolar, physiological levels of $O_2^{\cdot-}$ and its progeny. In a very elegant and comprehensible report by Buettner et al, a more complex role of MnSOD in establishing cellular redox environment and thus biological state of the cell was discussed based on thermodynamic and kinetic grounds [15, 16]. In addition to its traditional role in controlling levels of $O_2^{\cdot-}$ via catalysis of $O_2^{\cdot-}$ dismutation, MnSOD also modulates the accumulation of H_2O_2 in cells, most so effecting those $O_2^{\cdot-}$ - involving reactions whose equilibrium constant is $K < 1$, such as the production of superoxide from mitochondrial respiration at the site of coenzyme Q [15, 16].

Moreover, MnSOD influences the activity of transcription factors (such as HIF-1α, AP-1, NF-κB and p53) and affects DNA stability: an example being the action of overexpressed MnSOD on the maspin (mammary serine protease inhibitor) mRNA in MCF-7 breast cancer cells that results in decreased invasiveness [17]. Further, overexpresssion of MnSOD suppresses the activity of HIF-1α in MCF cells in a biphasic manner: at lower levels of MnSOD, HIF-1α levels are elevated, but are suppressed at higher MnSOD levels [18]. The biphasic influence of MnSOD on activation of HIF-1α is H_2O_2-dependent, as removal of peroxides reverses the effect [18]. While the same biphasic behavior has been observed in IL-1α expression, it has not been observed in the migration potential of HT-1080 cells [19]. Low levels of MnSOD are able to drive migration, and higher levels of MnSOD potentiate

the effects. Further, overexpression of MnSOD causes reduction of AP-1 transcriptional activity in MCF-7 cells, which is mediated through altered expression of the Jun family of AP-1 subunits [20]. In a DMBA/TPA skin carcinogenesis model, AP-1 activation was much higher in MnSOD-knock-out than in overexpressor mice [20]. Overexpression of MnSOD in MCF-7 cells diminishes NF-κB activity and expression of IL-1 and IL-6, both NF-κB responsive genes. MnSOD also modulates the transcriptional activity of p53 [21]. Finally, overexpression of MnSOD impedes aneuploidy in Lck-Bax38/1 mice [22, 23]. A recent study by Mesquita et al. on the life-span of *S. cerevisiae* further emphasizes a vital role of MnSOD in cell physiology. When yeast was stressed by caloric restriction or catalase inactivation, and H_2O_2 levels increased above physiological levels but did not reach toxicity, the yeast tried to adapt via H_2O_2-induced stress response and upregulated SODs, in particular MnSOD [24]. Similar hormesis effects are suggested to be operative in aging [24]. *Similarly, the modulation of $O_2^{\cdot -}$ levels and transcriptional activity observed with MnSOD were detected with Mn porphyrin-based SOD mimics* (see below, under *Mn porphyrins*).

An early report by Oberley and Buettner showed that many tumor types have low levels of MnSOD [25, 26], and overexpression of MnSOD was shown to suppress the tumorigenicity of human melanoma cells, breast cancer cells, and glioma cells, suggesting that MnSOD is a tumor suppressor gene in a wide variety of cancers [3–6]. Yet, Hempel et al. have presented data that show increased levels of MnSOD in different tumor types [19]. Additional increase of MnSOD level was found during progression of a tumor to the metastatic stage in head and neck, pancreatic, gastric, colorectal brain, and oral squamous cell carcinomas. Such apparently controversial data likely arise from the differences in the redox status of the tumors explored (Figure 1). Tumorigenesis and metastasis are strongly dependent on the intrinsic levels of reactive species, as well as external factors that would increase the production of reactive species. A “normal” cell which has low levels of MnSOD is susceptible to oxidative stress, which in turn may favor its progression to a tumor cell [19] (Figure 1). Further, studies with transgenic mice expressing a luciferase reporter gene under the control of human MnSOD promoter demonstrate that the levels of MnSOD in such already transformed cell were reduced prior to the formation of cancer [13, 27]. As transformed cell proliferates, it is possible that it fights oxidative stress by upregulating MnSOD, which might result in an imbalance between the superoxide and peroxide removing enzymes, resulting in turn in increased peroxide levels [15, 19, 28, 29]. Peroxide would then perpetuate oxidative stress by affecting a broad array of signaling pathways that promote malignancy and metastasis. The upregulation of NADPH oxidases would sustain or enhance H_2O_2 levels. Lower levels of MnSOD were found in prostate cancer, but an increase in circulating MnSOD positively correlated with tumor reoccurrence in the form of bone metastases [30]. Catalase levels are often decreased in a variety of tumors and expression appears to decrease further with progression of a metastatic disease [31]. Similar results have been reported for the Se-based H_2O_2-scavenging enzymes, glutathione peroxidase, peroxiredoxin, thioredoxin reductase and selenoprotein P plasma 1 [32–36]. Many malignant properties have been reversed by the co-expression of catalase [19]. Catalase overexpression protects cancer cells against the pro-oxidative effect of menadione and ascorbate [37]. Based on such report, MnSOD has been considered as both tumor suppressor and tumor promoter.

In the initial onset/proliferative stage of a tumor, MnSOD appears to be a tumor suppressor (Figure 1). Yet, once tumor progresses to a more aggressive and invasive phenotype and MnSOD is upregulated, the role of MnSOD is that of an oncogene, since MnSOD level positively correlates with enhanced metastasis [19, 38]. Further evidence for the role of MnSOD as an oncogene has been provided by studies showing that overexpression of MnSOD in aggressive cancers is related to the increased level of H_2O_2 [19]. However, the increased tumor peroxide levels that result in enhanced malignancy, might be more

accurately described as arising from a perturbed harmony between the actions of superoxide- and peroxide-removing enzymes as well as from changes in expression of other H_2O_2-producing systems such as NADPH oxidases, and not from the singular action of MnSOD. The impact of MnSOD overexpression on superoxide production from electron transport chain, mentioned above, would contribute to the increased H_2O_2 production also [16]. Recently a study by St. Clair group showed that suppression and subsequent restoration of MnSOD expression is mediated by p53 and Sp1 [38]. In an early stage of skin carcinogenesis, MnSOD is suppressed by decreased Sp1 binding to the *MnSOD* promoter, which is consistent with the fact that Sp1 is essential for the basal expression of MnSOD and basal *MnSOD* transcription [38]. However, as the tumor progresses in an environment of high oxidative stress, p53 activity is lost and MnSOD levels increase again creating conditions in which cancer cells survive and undergo metastasis [38]. Both the Sp1 binding to *MnSOD* promoter as well as the loss of p53 is likely mediated by the cellular redox status.

Finally, due to the enhanced oxidative stress, it is possible that MnSOD protein expression is upregulated, yet protein inactivated via oxidative modifications, and therefore its metastatic potential suppressed [39, 40]. Evidence from the site-directed mutagenesis studies indicate that His-30 is an important amino acid involved in the hydrogen bond network in the catalytic domain of MnSOD. The proteomic analysis of MnSOD from medulloblastoma cell line showed the presence of 2-oxo-histidine in His 30 and 31 residues [19]. Another mechanism of MnSOD inactivation is nitration of the protein tyrosine residue [39, 40]. A similar observation was recently published with respect to thioredoxin in a low-grade human prostate cancer tissue: though protein levels were increased, the thioredoxin activity was reduced [41]. It is therefore critical that conclusions are always based on both protein expression and its activity.

In summary, the opposing views of MnSOD as tumor suppressor (antioxidant) or oncogene (pro-oxidant) may possibly be reconciled based on the differences in the redox status of normal, transformed, tumor and metastatic cells (Figure 1). Much remains to be learned about the role of both MnSOD and its mimics under physiological and pathological conditions. For further discussion, see also the Special Issue of *Anti-Cancer Agents in Medicinal Chemistry*, on “SOD enzymes and their mimics in cancer: pro- *vs* anti-oxidative mode of action,” ACAMC, 2011 [14, 15, 19, 28, 29].

SOD mimics

The essential role of superoxide dismutases in maintaining healthy metabolism and rescuing diseased cells, the rising awareness of the key impact of oxidative stress in numerous diseases, and the essential role of mitochondria in cell metabolism have led to a three-decade long effort to synthesize SOD mimics, particularly those that target mitochondria. The first data appeared in the late 1970s on the ability of Fe porphyrin, FeTM-4-PyP^{5+}, to catalyze $O_2^{\cdot -}$ dismutation, via a two-step process (equations 1 and 2, where M stands for metal) alike the one operative with SOD enzymes [42]:

$$M^{III}P^{5+} + O_2^{\cdot -} \leftarrow ==== \rightarrow M^{II}P^{4+} + O_2 \quad [1]$$

$$M^{II}P^{4+} + 2\,H^+ + O_2^{\cdot -} \leftarrow === \rightarrow M^{III}P^{5+} + H_2O_2 \quad [2]$$

It is only logical that the first compound studied as an SOD mimic was a metal complex. With SOD enzymes (FeSOD, MnSOD, NiSOD, Cu, ZnSOD), the catalysis occurs at the redox active metal site, which is able to easily accept and donate electrons and thus oxidize and reduce $O_2^{\cdot -}$. Iron porphyrin was the first metalloporphyrin explored, as iron is the active

site of numerous enzymes whose functions are redox-based. The examples are the *cyt* P450 family of enzymes, nitric oxide synthases, cyclooxygenases, and prolylhydroxylases. The reason for utilizing a metalloporphyrin as an active site is the cyclic nature of the porphyrin ligand which forms a metal complex of extreme stability, and thus assures the integrity of the metal site. Exploration of Mn porphyrins followed. Relative to Fe porphyrins, they have been considered more favorable agents for $O_2^{\cdot-}$ removal, as they preclude the release of "free" iron, which could possibly result in a Fenton-based toxicity. Other metal complexes, such as Mn salen derivatives, Mn cyclic polyamines, metal corroles, metal salts, metal oxides, Pt nanoparticles and non-metal compounds such as nitrones and nitroxides as well as natural products, have also been explored for their ability to catalytically remove $O_2^{\cdot-}$ (Figures 2 and 3), and were discussed in details elsewhere [27, 43–46]. Among the synthetic compounds, nitrones and nitroxides are not able to catalytically scavenge superoxide, whereas they are able to react with peroxynitrite. The oxoammonium cation, formed during one-electron oxidation of nitroxide, can in turn react with $O_2^{\cdot-}$, completing the "catalytic" cycle. Low-molecular Mn complexes with carboxylates have also been explored, as nature utilizes manganese as a substitute for superoxide dismutase [47–50]. Further, such studies are valuable because most high-molecular weight Mn complexes could release Mn, when cycling from a stable, higher +3 oxidation state to a less stable lower +2 oxidation state of Mn, during the two steps of a dismutation process. Among metal complexes, cationic Fe and Mn porphyrins bearing *meso* cationic pyridyl substituents, appear to have the highest catalytic rate constant for $O_2^{\cdot-}$ dismutation, $k_{cat}(O_2^{\cdot-})$. Thos compounds, which are substituted with electron-withdrawing groups on both *beta* and *meso* positions of porphyrin ring (Figure 2 and Figure 7), have the highest k_{cat}, nearing that of the enzyme itself. The most potent (yet unstable as it carries Mn in lower +2 oxidation state with insufficient charge density for complexing porphyrin ligand strongly enough) is the Mn(II) β-octabromo-*meso*-tetrakis(*N*-methylpyridinium-3-yl)porphyrin, $MnBr_8TM\text{-}3\text{-}PyP^{4+}$ (Figure 7, Table 1), whose log k_{cat} is ≥8.85, while SOD has the log k_{cat} in between 8.84 and 9.30 [45]. Yet, the complex is unstable as it carries Mn in a lower +2 oxidation state, which has insufficient charge density to bind porphyrin ligand strongly enough. With no β-substituents, the Mn(III) *N*-alkylpyridylporphyrins are stable complexes (even in 36% hydrochloric acid), and have a log k_{cat} ranging from 6.58 to 7.79. A comprehensive overview of different classes of SOD mimics has been reported recently [44–46].

MnSOD mimics

Increased understanding of the role of mitochondria and its enzyme, MnSOD, has motivated researchers to explore existing and new compounds for their ability to enter mitochondria and mimic MnSOD. This review covers only those compounds that reportedly possess fair SOD-like properties (are catalysts of $O_2^{\cdot-}$ dismutation), or are stoichiometric scavengers of $O_2^{\cdot-}$, and for which evidence exists that they are efficacious in attenuating mitochondrial dysfunction. Mn porphyrins and $MitoQ_{10}$ are addressed in this report in detail, as there is substantial evidence that they accumulate in mitochondria and possess high rate constants for reaction with $O_2^{\cdot-}$. Both types of compounds bear a cationic charge (shown by Liberman, Skulachev and Murphy to be a driving force for drug accumulation in mitochondria) and a redox-active unit [51–53]. Singly-charged $MitoQ_{10}$ is more lipophilic than either of the pentacationic Mn porphyrins studied; it seems that, at least in part, the multiple charge of Mn porphyrins compensates for their much lower lipophilicity when compared to $MitoQ_{10}$. Mn cyclic polyamine-based SOD mimics and the most potent compounds within the class of redox-active corroles lack positive charge or are anionic compounds, respectively; their mitochondrial accumulation would thus be disfavored. No evidence has yet been provided that these compounds reach mitochondria [46, 54].

MnSOD-plasmid liposome gene

The natural way to compensate for MnSOD is to use MnSOD itself in a bioavailable form – MnSOD-plasmid liposome gene. Such therapy has been shown to decrease irradiation-induced lipid peroxidation of the mouse esophagus [55].

The attachment of mitochondria-targeted amino acid sequence to a Mn porphyrin-based SOD mimic

The Asayama et al attached a mitochondria-targeted amino acid sequence to a Mn porphyrin-based SOD mimic, MnTM-4-PyP^{5+} (Figure 2) [56]. By using the pH-sensitive aminated poly(L-histidine) drug carrier for intracellular delivery, the new conjugate recovered the viability of lipopolysaccharide (LPS)-stimulated macrophage RAW 264.7 cells.

Pyrroloquinoline quinone (PQQ)

(Figure 3) is a water-soluble redox cycling orthoquinone, a nutrient widely distributed in nature. It serves as a non-covalently bound redox cofactor in a series of bacterial quinoprotein dehydrogenases and has been explored for treatment of mitochondrial disorders [57]. In the presence of reductants, PQQ scavenges ROS in bacteria [58]. PQQ protects isolated liver mitochondria from oxidative damage, *via* superoxide scavenging, and was neuroprotective in a rodent stroke model where its action was assigned to peroxynitrite scavenging [57–63]. PQQ also reduces myocardial infarct size, improves cardiac function, and reduces lipid peroxidation as measured by malondialdehyde levels [64, 65].

MnSalens

While not significantly efficacious in a cellular model of ataxia telangiectasia, MnSalen, EUK-8 (Figure 2) was very efficacious in the protection of the MnSOD-knock out yeast *Cryptococcus neoformans* against heat-mediated injury [66]. Neither cationic nor anionic Mn porphyrins were efficacious. Also, Tempol and $MnCl_2$ lacked efficacy. EUK-8 is a fairly unstable complex and loses Mn in the presence of EDTA [67]. Therefore, *in vivo*, MnSalen perhaps serves as a Mn transporter into mitochondria. Cationic Mn(III) *N*-alkylpyridylporphyrin complexes are too strong to release manganese. MnTBAP^{3-} carries a triple negative charge and thus cannot easily reach mitochondria. Furthermore, it is too stable to release Mn there, and is not SOD mimic in its own right [68]. Data on *C. neoformans* justify further exploration of MnSalen derivatives. Irradiated astrocytes have been shown to develop mitochondrial abnormalities attenuated in a dose-dependent manner by EUK-134. Vorotnikova et al. showed that EUK-207 and EUK-189 inhibit radiation-induced apoptosis in bovine adrenal endothelial cells [69]. A study on life-span extension and rescue of spongiform encephalopathy in MnSOD$^{-/-}$ mice showed that EUK-8 mimics MnSOD. Yet, that report has been questioned by Keaney et al. [70, 71].

MnMImP$_3$P^{2+}

The Mn(III) porphyrin, MnMImP$_3$P^{2+}, depicted in Figure 2, reportedly targets mitochondria [72]. When compared to its fully ethylated analogue MnTDE-2-ImP^{5+}, the compound has only one imidazolium ring fully methylated, and thus carries 2 instead of 8 methyl groups. Consequently, MnMImP$_3$P^{2+} bears only 2+ instead of 5+ total charges, has therefore reduced antioxidant potency, but increased lipophilicity than MnTDE-2-ImP^{5+} (Table 1). The inferior SOD-like activity of MnMImP$_3$P^{2+} is at least in part compensated by its fair lipophilicity (log P_{OW} = 4.78), which in turn favors its mitochondrial accumulation.

Nitroxides

Nitroxides (Figure 3) are weak SOD mimics [46]; their SOD activity increases with a pH drop due to their high reactivity with protonated superoxide, HO_2; the $RNO^{\cdot}/RNO^{+}$ redox couple is involved [46]. Nitroxides, $RNO^{\cdot}$ can be oxidized to oxoammonium cation, RNO^{+} with $ONOO^{-}$ (Table 1), which in turn rapidly reacts with $O_2^{\cdot -}$ regenerating $RNO^{\cdot}$; thus, the catalytic removal of $O_2^{\cdot -}$ may be coupled to the reaction with $ONOO^{-}$. *In vivo* nitroxides, $RNO^{\cdot}$ are reduced to hydroxylamine, RNOH, which reportedly acts as an antioxidant [73]. The lipophilic keto analogues, tempone and oxazolidine-5-doxylstearate (but not hydrophilic tempol), are reduced by mitochondria of intact cells, which indicates the ability of nitroxide to reach these cellular components. While nitroxides are uncharged, nitrones such as PBN carry an anionic charge. Therefore, PBN may localize in mitochondria only after reacting with free radicals, thereby losing its anionic charge [74]. 5,5-dimethyl-1-pyrroline-1-oxide, DMPO, a spin trapping agent, reportedly enters mitochondria, where it is reduced by the electron-transport chain of mitochondria of synaptosomes [75].

Mangafodipir

A Mn complex with dipyridoxyl diphosphate (Figure 2), a MRI contrast agent for liver and cardiac imaging, has been shown to improve contractile function and reduce enzyme release in rat heart tissue during reoxygenation, and could be used as a viability marker in patients with myocardial infarction. It has also been shown to reduce mitochondrial damage by reducing reactive species, presumably mimicking superoxide dismutase [76], catalase and glutathione reductase [77].

Mitochondria- targeted peptide

Other compounds that possess the ability to scavenge reactive species, but that have no SOD-like activity, have also been developed. An example is the mitochondrially-targeted peptide that contains dimethyltyrosine unit (Dmt), which reportedly scavenges reactive species [78, 79]. The unique feature of SS-02 (H-Dmt-D-Arg-Phe-Lys-NH_2) is its alternating aromatic-cationic structural motif, where aromatic residues (Dmt and Phe) alternate with basic residues (Arg and Lys). This motif allows for intramolecular cation-π interaction between the electron-rich π ring (Dmt or Phe) and the adjacent cation (Arg or Lys). The additional methyl groups on Dmt further increase electron density on the π ring. Cation-π energies are of the same order of magnitude as hydrogen bonding energies, and the π rings may shield the cation charge and enhance membrane penetration. Thus, this aromatic-cationic motif is retained in the design of non-opioid analogs of SS-02. Reactive nitrogen and halogen species, $^{\cdot}OH$ and $RO_2^{\cdot}/RO^{\cdot}$ [80], are known to target tyrosine, thereby producing dihydroxyphenylalanine and tyrosine radicals. Tyrosine radicals would form dityrosine, a reaction that is facilitated by $O_2^{\cdot -}$ [81]. While substitution of dimethyltyrosine with phenylalanine resulted in a loss of antioxidant capacity, the peptide was still able to reduce ROS generation [78, 79]. It must be noted that formation of tyrosine radical is usually associated with the oxidative damage of protein which, in the presence of $ONOO^{-}$, would lead to nitrotyrosine formation. This modification is known to inactivate MnSOD [39, 40]. Beneficial effects of the mitochondrially-targeted peptide have been observed with disorders that have mitochondrial dysfunction in common, such as neurodegenerative diseases, metabolic syndrome, muscle atrophy and weakness, heart failure, and ischemia-reperfusion injuries.

Manganese and its complexes with simple ligands

Evidence suggests that MnSalen, EUK-8 and $MnBr_8TM\text{-}3\text{-}PyP^{4+}$ transport Mn into the mitochondria of *C. neoformans* and into the cytosol of *E. coli*, respectively [29, 82]. One of the hypotheses is that mitochondria of eukaryotic cell have evolved from bacteria [83].

Thus, the data related to the cytosol of prokaryotic *E. coli* are relevant to the mitochondrial matrix of *C. neoformans*. In MnSOD-knockout *C. neoformans*, MnSalen or the Mn released in mitochondria from its complex have been shown to substitute for the lack of MnSOD (see also under MnSalens [66]). *Lactobacillus plantarum* accumulates Mn to milimolar levels as a protection against oxidative stress [47]. Expressed per milligram of Mn, the SOD-like activity of Mn(II) lactate is 65-fold lower than that of SOD enzymes [46]. Mn^{2+} protects *E. coli* when growing aerobically at > 0.5 mM [84], and exogenous Mn millimolar concentrations rescued $O_2^{\cdot-}$ - sensitive phenotype of *S. cerevisiae* lacking Cu, ZnSOD [46, 50, 85, 86]. Finally, Mn^{2+} accelerates wild type development, enhances stress resistance and rescues the life span of a short-lived *Caenorhabditis elegans* mutant [87].

MitoQ$_{10}$

The Liberman, Skulachev and Murphy group [49–51] clearly established that both positive charge and lipophilicity play critical roles in a molecule intended for mitochondrial targeting. Thus both features were incorporated into the design of MitoQ$_{10}$. The compound was developed to enter cells driven by plasma membrane potential, and mitochondria driven by mitochondrial membrane potential. In MitoQ, a redox-cycling quinone, an analogue of the ubiquinone of the mitochondrial electron transport chain, was coupled to a cationic triphenylphosphonium ion via long lipophilic alkyl chain [89]. The longer the alkyl chain, the higher is the mitochondrial accumulation of MitoQ [89]. An optimized MitoQ$_{10}$ molecule, with a 10-carbon atom-alkyl chain, has the capacity to suppress mitochondrial oxidative stress (Figure 3). In animals and cells, MitoQ$_{10}$ is rapidly reduced two-electronically by the mitochondrial respiratory chain to quinol, MitoQH$_2$, which is stable over a long-term incubation. The reduction is essential for the compound to act as a reducing agent/antioxidant. The major metabolite detected *in vivo* is monosulfonated MitoQ$_{10}$, which upon loss of sulfonate regenerates MitoQH$_2$ [93].

The reactivity of MitoQ$_{10}$ toward $O_2^{\cdot-}$ and other oxygen radicals has been studied in detail [94]. MitoQ$_{10}$ reacts with $O_2^{\cdot-}$ in water and methanol with rate constants of 2.0×10^8 $M^{-1}s^{-1}$ and 4.2×10^8 $M^{-1}s^{-1}$, respectively, forming semiquinone radical, MitoQH$^{\cdot}$, which then dismutes (disproportionates) to MitoQ$_{10}$ and quinol, MitoQH$_2$. Also, MitoQH$^{\cdot}$ reacts with O_2 in a reverse reaction with rate constants of 2.9×10^7 $M^{-1}s^{-1}$ and 7.3×10^8 $M^{-1}s^{-1}$ in water and methanol, respectively (Figure 4). The forward reaction is 10-fold more preferred over the backward. The $E_{1/2}$ for $O_2/O_2^{\cdot-}$ couple is −155 mV *vs* NHE and −630 mV *vs* NHE in water and aprotic solvents, while it is −105 mV *vs* NHE and −415 mV *vs* NHE for the mitoQ/ubisemiquinone in water and UQ/UQH$^{\cdot}$ in aprotic solvents, respectively [94]. The reaction of $O_2^{\cdot-}$ with MitoQH$_2$ is insignificant, with a rate constant of $\ll 10^5$ $M^{-1}s^{-1}$. MitoQH$_2$ (but not MitoQ quinone), resides in the hydrophobic core of membrane, where it can react with protonated $O_2^{\cdot-}$ ($HO_2^{\cdot}$) with a rate constant of ~10^6 $M^{-1}s^{-1}$ (Figure 4). Thus, catalysis of $O_2^{\cdot-}$ dismutation may be achieved via coupling of MitoQ$_{10}$/MitoQH$_2$ with other reactive species and components of the electron-transport chain.

Reactivities of MitoQ$_{10}$ toward other species

MitoQH$_2$ rapidly reacts with $ONOO^-$ (whereby MitoQH$^{\cdot}$ is produced, which then undergoes dismutation [89]) and is particularly effective against lipid peroxidation [89]. Similar to other redox-able compounds, MitoQ$_{10}$ affects cellular transcriptional activity, presumably by modulating levels of cellular signaling species [53]. It blocks H_2O_2-induced apoptosis and cell death, but the mechanism is not fully understood. Further, a partially reduced form of MitoQH$^{\cdot}$ (semiquinone) can act as a pro-oxidant. As is the case with Mn porphyrins (see below) and many other redox-active compounds [44, 95], MitoQ$_{10}$ can act *in vivo* as a pro-oxidant, which in turn could result in an adaptive response and in upregulation of endogenous antioxidant defenses [89].

Mitochondrial accumulation of $MitoQ_{10}$

$MitoQ_{10}$ distributes predominantly into mitochondria [93]. In both cytosol and mitochondria, $MitoQ_{10}$ is bound and essentially no free compound is found. With energized mitochondria, $MitoQ_{10}$ is most likely bound at the matrix-facing surface of the inner membrane, with the triphenylphosphonium cation in a potential energy well close to the surface. The hydrophobic side chain is inserted into the membrane [96].

$MitoQ_{10}$ analogues

Due to the necessity to treat mitochondrial dysfunction, numerous modifications of $MitoQ_{10}$ based on the original design were subsequently reported. Instead of quinone, such derivatives bear vitamin E (Mito-αToc), dihydroethidium (MitoSOX™ Red [97]), nitroxide (Mito-Tempol, Mito-CP and Mito-CTP) [98, 99], ebselen (a mimic of glutathione peroxidase), MnSalen [99], ·NO donor (MitoSNO [100]), and boronic acid peroxide sensor (MitoB [101]). MitoSOX™ Red, where redox- able moiety is dihydroethidium (a stoichiometric scavenger of $O_2^{\cdot -}$), has been widely utilized as a mechanistic tool to prove the involvement of mitochondrially produced superoxide in oxidative stress [102]. Caution needs to be exercised as the effect of Mito moiety on cellular bioenergetics was reported [103].

Therapeutic effects of $MitoQ_{10}$

The compound has thus far been employed in numerous studies and has already proven efficacious in animal models of oxidative stress, such as type I diabetes nephropathy, cold storage of renal cells and kidneys, cardiac ischemia/reperfusion, endotoxin-induced cardiac dysfunction, doxorubicin-induced cardiac toxicity, protection against increase in blood pressure in spontaneously hypertensive rats, and prevention of amyloid β-induced impairments in hippocampal synaptic plasticity in wild-type hippocampal slices treated with exogenous amyloid β peptide. It has been also tested in two phase-II clinical trials [104]. $MitoQ_{10}$ was tested on its ability to slow down Parkinson's disease progression, where no difference was seen between placebo and $MitoQ_{10}$ groups. The study provides important safety data for long-term administration to humans. In a chronic liver hepatitis study of HCV-infected patients, efficacy in decreasing serum alanine transaminase was observed, but no effect on viral load was observed [104]. $MitoQ_{10}$ has 10% oral availability. Oral dosing to humans at 80 mg (1mg/kg) results in maximal plasma levels of 33.15 ng/mL at 1 hour.

Mn porphyrins

Optimization of k_{cat} ($O_2^{\cdot -}$), bioavailability and toxicity

Mn porphyrins are among the most potent and true catalysts of $O_2^{\cdot -}$ dismutation, with k_{cat} reaching the potency of SOD enzymes. They have been designed to mimic the action of the enzyme catalytic site. The detailed chemistry, biochemistry and biology of Mn porphyrins have been reviewed recently [44–46], and are briefly summarized below with most recent data included.

The reduction potential of the metal site of the enzyme, regardless of the type of metal (Cu, Mn, Fe or Ni), is around the midway (~ +300 mV *vs* NHE), between the potential for oxidation (−160 mV *vs* NHE) and the reduction of superoxide (+890 mV *vs* NHE) (Figure 5). Therefore, both steps of the catalytic cycle are equally favored thermodynamically; consequently, both oxidation and reduction of $O_2^{\cdot -}$ by enzyme occur with the identical rate constant of $\sim 2 \times 10^9\ M^{-1}\ s^{-1}$ [105–107]. Further, dismutation is electrostatically facilitated, as the superoxide anions are pulled toward the metal center through a tunnel encircled with positively charged amino acids [108]. We attempted to derivatize metalloporphyrins by mimicking the thermodynamics and electrostatics of the enzyme catalysis. The unsubstituted

porphyrins have $E_{1/2}$ for the Mn^{III}/Mn^{II} redox couple ~ −200 to −300 mV *vs* NHE and cannot be reduced with $O_2^{\cdot-}$ in the step one of the dismutation process (eq.1); the metal site reduction was a rate-limiting step (Figure 5) [82, 109]. In order to make the metal site more reducible, the electron-withdrawing groups were attached to the porphyrin ring in *meso* and *beta* positions which resulted in a significant increase in Mn electron-deficiency which translated into a significant increase in $E_{1/2}$. Across the wide range of compounds thus far synthesized and commercially obtained, the $E_{1/2}$ was increased by up to ~ 800 mV relative to unsubstituted Mn porphyrins; the $MnCl_5TE\text{-}2\text{-}PyP^{4+}$ has the highest $E_{1/2}$ of +560 mV *vs* NHE [46]. Based on compounds explored, the structure-activity relationship (SAR) was originally established [110], and later revised (Figure 6). SAR shows that as the $E_{1/2}$ increases, the k_{cat} increases as well. At $E_{1/2}$ ~ +200 mV, both steps of the dismutation process occur with similar rate constants [109].

As $E_{1/2}$ becomes more positive and increases beyond +400 mV *vs* NHE, the metal site becomes so electron-deficient that it gets stabilized in +2 oxidation state. Examples are Mn(II) complexes, $MnBr_8TM\text{-}3(\text{and }4)\text{-}PyP^{4+}$ and $MnCl_5TE\text{-}2\text{-}PyP^{4+}$ (Table 1) [44–46]. These compounds are not stable enough under physiological pH conditions and readily lose metal. They are, however, excellent mechanistic tools, proving that even a simple porphyrin ligand could be modified to achieve the catalytic potency of a protein structure. Further increase in $E_{1/2}$ would stabilize Mn +2 oxidation state so much that the oxidation of a metal complex would become unfavorable; i.e. the oxidation of Mn porphyrin would become a rate-limiting step (eq. 2). Thus, such complexes would be poor SOD mimics also. Based on SAR, the *ortho* isomeric cationic Mn(III) *N*-alkylpyridylporphyrins were identified as the most efficacious SOD mimics thus far synthesized (Figure 6). Figure 6 further clearly shows that at $E_{1/2}$ ~ +200 mV the cationic Mn porphyrins are ≥100-fold more potent than compounds that have no charge or possess anionic charges on their periphery [44–46]. Such data point to the crucial impact of electrostatics on the catalysis of $O_2^{\cdot-}$ dismutation by MnPs. In summary, the exploration of the design of SOD mimics shows that *ortho isomeric compounds possess a key property that is essential for their ability to catalyze* $O_2^{\cdot-}$ *dismutation: electron-withdrawing cationic pyridyl nitrogens close to the Mn site which (1) make the Mn(III) site electron-deficient and thus eager to accept electrons from the superoxide in the first step of the dismutation process; and (2) attract anionic superoxide toward the singly charged Mn site.*

The timeline for the optimization of SOD mimics is depicted in Figure 7. In Phase I we aimed at designing compounds whose $k_{cat}(O_2^{\cdot-})$ approaches that of an enzyme. As our research progressed, it became clear that the efficacy *in vivo* would also depend on the lipophilicity of the compound, as well as on its bulkiness, size, and shape (Figure 7). The latter properties may hinder the cationic charges and thus suppress the unfavorable approach of the compound to the targeted biological molecules and thus decrease MnP toxicity. For example, the interaction of cationic charges of the more planar *para* isomer, $MnTM\text{-}4\text{-}PyP^{5+}$ with nucleic acids, precludes the approach of $O_2^{\cdot-}$ to the Mn site, and in turn leads to the complete loss of its SOD-like activity *in vivo*. Further, with cationic MnPs, a blood pressure drop, as a side effect, was found in animal studies [44–46]. The effect is lower with $MnTnHex\text{-}2\text{-}PyP^{5+}$ than with $MnTE\text{-}2\text{-}PyP^{5+}$, presumably due to the larger hindrance of cationic charges by longer alkyl chains [112, 113]. Yet, in certain cases the hindrance of charges may be unfavorable. For example, the cationic charges may favor the approach of Mn porphyrin to the deprotonated anionic cysteine residues of signaling proteins such as p50 and p65 subunits of NF-κB, and thus facilitate the cysteine oxidation or glutathionylation, respectively, which in turn would prevent NF-κB DNA binding and suppress excessive inflammation [27, 114, 115].

The first potent porphyrin-based SOD mimics, MnTM-2-PyP^{5+} and MnTE-2-PyP^{5+} (Figure 1), were developed 15 years ago. Based on the same principles, di-*ortho* imidazolium analog, MnTDE-2-ImP^{5+}, was subsequently synthesized. Because these compounds are fairly hydrophilic and bear total pentacationic charge, it seemed at first unlikely that they would cross the blood brain barrier (BBB) and target mitochondria. In an effort to facilitate transport across the BBB and enhance accumulation within mitochondria, we have optimized the properties of the cationic porphyrin by lengthening the alkyl chains of *meso* pyridyl groups. While maintaining the total cationic charge, and therefore the redox activity, we synthesized lipophilic Mn porphyrins with longer hydrophobic alkyl chains: MnTnHex-2-PyP^{5+} and MnTnOct-2-PyP^{5+}. We subsequently showed that: (1) a number of carbon atoms in alkyl chains are proportional to MnP lipophilicity (the increase in alkyl chain length for one carbon atom increases MnP lipophilicity 10-fold) (Table 1) [91]; and (2) lipophilic members accumulate more in *E. coli* and exert their efficacy at significantly lower doses than hydrophilic analogs do [91, 116]. MnTnHex-2-PyP^{5+} and MnTnOct-2-PyP^{5+} are ~10,000- and 300,000-fold more lipophilic than MnTE-2-PyP^{5+} [44–46]. Such a remarkable gain in lipophilicity translates into a more than 3-orders of magnitude increased *in vivo* efficacy of lipophilic Mn porphyrins. Their therapeutic superiority is detailed below under "*The* in vitro *and* in vivo *efficacy of Mn porphyrins.*"

We have originally limited ourselves to the study of *ortho* isomeric Mn(III) *N*-alkylpyridylporphyrins as they have the highest $k_{cat}(O_2^{\cdot-})$ among MnPs studied. Yet, our growing insight into the magnitude of the effect of lipophilicity upon *in vivo* efficacy tempted us to revisit the 10-fold more lipophilic *meta* isomers. A nice set of data obtained in an *E. coli* study shows that higher bioavalibility of a MnP can markedly compensate for its inferior redox potency. The *meta* isomer MnTE-3-PyP^{5+} has a 10-fold lower SOD potency, but is 10-fold more lipophilic than *ortho* MnTE-2-PyP^{5+}. In turn, MnTE-3-PyP^{5+} accumulates at 10-fold higher levels within *E. coli* cell than MnTE-2-PyP^{5+}. Consequently, both compounds are equally able to protect SOD-deficient *E. coli* strain when growing aerobically [91].

The toxicity of cationic Mn(III) alkylpyridylporphyrins is at least in part due to their micellar character, which arises from their polar cationic nitrogens and hydrophobic alkyl chains (Figure 7). Our most recent efforts have been directed toward reducing the toxicity of the lipophilic longer alkyl-chain analogs. Two strategies were applied. Firstly, oxygen was introduced at the end of each alkyl chain [109, 117]; however this strategy significantly reduced MnP lipophilicity. The second approach was to bury oxygen atoms deep into each of the alkyl chains, thus closer to the pyridyl nitrogens [118]; such strategy preserved the lipophilicity and the SOD-like potency of MnP, while largely diminishing its toxicity.

Accumulation of Mn porphyrins in mitochondria

The excessive pentacationic charge of MnTE-2-PyP^{5+} set initial doubts on its ability to enter mitochondria and cross the BBB. However, it was shown by Liberman, Skulachev's and Murphy's groups that cationic charge has a critical role in driving drug mitochondrial localization [51]. The St. Clair group recently showed that cationic MnTE-2-PyP^{5+} reduces incidence and multiplicity of papillomas in a mouse skin carcinogenesis model in a manner similar to MnSOD enzyme (see details under *Skin carcinogenesis*) [119]. The data therefore suggest that the MnP ends up in mitochondria and more specifically in the mitochondrial matrix. Concurrently, Ferrer-Sueta et al. showed that ≥ 3 μM MnTE-2-PyP^{5+} protects submitochondrial particles against oxidative stress imposed by peroxynitrite [120]. Subsequently, we quantified the accumulation of MnTE-2-PyP^{5+} in mouse heart mitochondria: at 5.1 μM, its levels are high enough to protect mitochondria against oxidative damage [121].

Mouse heart studies

To test the hypothesis that lipophilicity has a critical impact on the mitochondrial targeting of Mn porphyrins, we performed a mouse study on MnTnHex-2-PyP^{5+}. The data are discussed in relation to the mitochondrial accumulation of ~10,000-fold less lipophilic MnTE-2-PyP^{5+} (Figure 2, Table 1) [121]. MnTnHex-2-PyP^{5+} was given ip at a maximal tolerable single dose of 2 mg/kg, while MnTE-2-PyP^{5+} was given ip at 10 mg/kg. The *in vivo* levels of MnPs were determined as previously described, employing the LC/ESI-MS/MS method [45, 122]. MnTE-2-PyP^{5+} was found in mouse heart mitochondria at (2.95 ± 1.24) ng/mg protein [121], and MnTnHex-2-PyP^{5+} was found at (12.17 ± 8.48) ng/mg protein. Given the average value of mitochondrial volume of 0.6 μL/mg protein [123–130], the concentration of MnTE-2-PyP^{5+} in mitochondria was 5.1 μM, while it was 21.0 μM in the case of MnTnHex-2-PyP^{5+}. The data are normalized to mg of drug injected and show that *MnTnHex-2-PyP^{5+} accumulates ~20-fold more in mitochondria than does MnTE-2-PyP^{5+}* (Figure 8B). When cytosolic and mitochondrial fractions are compared, MnTnHex-2-PyP^{5+} [121] accumulates ~5-fold more in mitochondria than in cytosol (Figure 8). The study supports the key impact of lipophilicity on the transport of MnP into cells and its accumulation in mitochondria.

S. cerevisiae studies

The mouse cardiac data parallel the data generated with *S. cerevisiae*. The accumulation of MnPs within mitochondria is proportional to the compound lipophilicity, which in turn is proportional to the length of porphyrin alkyl chains [122, 131]. The compound bearing methyl (M) chains, MnTM-2-PyP^{5+} distributes evenly between yeast mitochondria and cytosol, MnTE-2-PyP^{5+} resides 2–3-fold more in mitochondria than in cytosol, while the MnTnHex-2-PyP^{5+} is ≥ 90% in mitochondria [122, 131].

E. coli studies

One of the hypotheses is that eukaryotic cell mitochondria are evolutionarily derived from bacteria [83]. Thus the *E. coli* membranes/wall (envelope) and cytosol may be viewed as analogous to the mouse mitochondrial membranes and matrix, respectively. Not surprisingly, therefore, the mouse mitochondrial data are in excellent agreement with the accumulation of cationic Mn porphyrins in *E. coli* [91] (Figure 8C). The accumulation was followed in both SOD-deficient and wild strains of *E. coli*. The accumulation was higher in the SOD-deficient strain, where MnPs exerted a remarkable ability to substitute for the lack of cytosolic MnSOD and FeSOD [45, 91]. In agreement with the mouse heart studies, the lipophilic member of the porphyrin series, MnTnHex-2-PyP^{5+}, resides at ~30-fold more in envelope and 100-fold more in the cytosol of *E. coli* than MnTE-2-PyP^{5+} (Figure 8C). *E. coli* data further show that all MnPs tend to distribute more in envelope than in the cytosol (Figure 8C). While MnTnHex-2-PyP^{5+} accumulates twice more in envelope than in cytosol, MnTE-2-PyP^{5+} distributes 10-fold more in envelope than in cytosol. The *E. coli* data also suggest that in addition to the mitochondrial matrix, MnTnHex-2-PyP^{5+} could reside within mouse cardiac mitochondrial membranes, and/or be placed at the inner membrane/matrix interface, where the lipophilic chains may be stuck within the membrane while cationic heads reach the matrix (similar to MitoQ$_{10}$). It can thus mimic both isoforms of mitochondrial enzymes: MnSOD and Cu, ZnSOD. Further studies are needed to address the compartmentalization of MnTnHex-2-PyP^{5+} within mitochondria.

Accumulation of Mn porphyrins in brain

The critical effect of lipophilicity of MnPs upon their *in vivo* action is further evidenced in those animal studies where transport across BBB is required for their efficacy (stroke, subarachnoid hemorrhage, pain, cerebral palsy, neurologic disorders, etc) [42–44]. The

hydrophilic MnTE-2-PyP^{5+} accumulates in brain over a 7-day period after a single 10 mg/kg ip injection [121]. As expected, MnTnHex-2-PyP^{5+} accumulates in brain at ~9-fold higher levels [112], which agrees with its 20-fold higher mitochondrial accumulation (Figures 8 and 9). Such agreement is due to the fact that in both cases the ability of MnP to cross lipid membranes plays a major role.

Accumulation of Mn porphyrins in tumor tissue

The first set of data on MnP accumulation in tumors was obtained in a 4T1 mouse breast cancer model where MnTnHex-2-PyP^{5+} was administered during the duration of experiment twice daily ip at 1.6 mg/kg with and without sodium ascorbate [132]. The Mn porphyrin accumulated ~5-fold more in tumor (sc xenografts were established on right flank) than in the muscle taken from the left leg [132]. The enhanced accumulation in tumor relative to muscle was observed when mice were treated either with MnP alone or with MnP/ascorbate. Combined administration with ascorbate is relevant due to the high levels of ascorbate *in vivo*, were MnP action is likely coupled to ascorbate redox cycling. Other reductants, such as glutathione, tetrahydrobiopterin and protein cysteine residues, may be also involved in MnP reduction (from Mn^{III}P to Mn^{II}P) and its redox-cycling [44, 114, 115, 133]. Once reduced, MnP loses a single charge from the Mn site and in turn becomes more hydrophobic [132]. The gain in lipophilicity is related to the length of porphyrin alkyl chains in a bell-shape fashion: ≥10-fold increase was found with MnTE-2-PyP^{5+} and MnTnHex-2-PyP^{5+} [132]. Such increased lipophilicity may enhance MnP subcellular accumulation. Most recent data on MRI imaging of prostate cancer, employing Mn porphyrins as contrast agents, show also that MnTE-2-PyP^{5+} distributes more in prostate tumor than in the surrounding tissue [134].

Mechanism of action of Mn porphyrins

Alike MnSOD enzyme, the Mn porphyrins affect levels of reactive species and activation of transcription factors, whereby acting as fine cellular redox modulators. These actions may be independent or related, as reactive species are both strong oxidants and also major signaling species. The MnP-based SOD mimics have been proven efficacious in numerous *in vitro* and *in vivo* models, and the efficacy was reproduced in various laboratories both within and outside the United States [13, 27, 44–46, 132].

Reactivity toward reactive species

Increased knowledge about the chemistry and biology of redox-active compounds and the role of reactive species and endogenous antioxidants makes it clear that synthetic SOD mimics as well as stoichiometric scavengers of superoxide are not specific towards $O_2^{\cdot -}$ (Figure 10). The possible reactions of Mn(III) *N*-alkylpyridylporphyrins are depicted in Figure 10 to point to the complexity of *in vivo* systems and to emphasize the need to further the knowledge on the biology of MnPs and cellular components and their mutual interactions. The diverse reactivities of MnPs make mechanistic studies more challenging, requiring multiple controls and genetic tool to single out the predominant species involved.

While mechanistic aspects need further exploration, the beneficial therapeutic effects are obvious because the *failure to remove $O_2^{\cdot -}$ by MnP would result in increased levels of its progeny, such as, $^{\cdot}OH$, $ONOO^-$, $^{\cdot}NO_2$, $CO_3^{\cdot -}$, and lipid peroxyl radicals. Thus, the potent MnP-based SOD mimics would efficiently suppress not only the levels of $O_2^{\cdot -}$ but of all species originated from it.*

The electron-deficient metal porphyrin center favors binding of the anionic $ONOO^-$ to Mn(III) or Mn(II) (reduced by cellular reductant or $O_2^{\cdot -}$), which is followed by the one-electron or two-electron reductions of $ONOO^-$ to $NO_2^{\cdot}$ or NO_2^-, respectively [135, 136].

Reduction of $CO_3^{\cdot-}$ by MnPs and reactivity toward $^{\cdot}NO$ have also been reported (Figure 10A). Further, preliminary data [Ferrer-Sueta et al., unpublished] indicate that MnPs have high ability to reduce ClO^-. Reduced Mn(II) porphyrins have fairly high reactivity towards molecular oxygen as well (Figure 11). Among the rate constants thus far determined, the highest are those related to the elimination of $O_2^{\cdot-}$ and $CO_3^{\cdot-}$, followed by $k_{red}(ONOO^-)$ [44–46, 136]. The type of reaction favored *in vivo* will ultimately depend upon the levels of MnPs, reactive species, cellular reductants and their co-localization with MnPs.

Mn porphyrins and cellular reductants

Electron deficiency of a Mn site facilitates easy reduction of Mn porphyrins not only with $O_2^{\cdot-}$ but with cellular reductants, such as ascorbate, glutathione, tetrahydrobiopterin and flavoproteins of mitochondrial respiration. As those reductants are highly abundant *in vivo*, the removal of $O_2^{\cdot-}$ by MnPs would likely be coupled with redox cycling of ascorbate or glutathione [133, 138, 139]. Thus, in a first step, ascorbate would reduce $Mn^{III}P$ to $Mn^{II}P$. Subsequently, the $Mn^{II}P$ would reduce $O_2^{\cdot-}$ to H_2O_2. Consequently, MnPs may *in vivo* act as superoxide reductases rather than superoxide dismutases [140].

MnPs could *in vivo* increase levels of H_2O_2 either *via* catalysis of $O_2^{\cdot-}$ dismutation or reaction of $Mn^{II}P$ with O_2, or *via* catalysis of ascorbate oxidation (Figure 11), but only if the cellular levels of peroxide-removing enzymes are reduced and therefore the physiological redox status perturbed. The scenario where MnP may drive H_2O_2 production from electron transport chain, as discussed for MnSOD enzyme by Buettner et al [16] (see Introduction), might be operative as well. We and others have shown in different cancer cell lines that, in the presence of exogenous ascorbate, MnPs catalyze ascorbate oxidation, and in turn increase levels of H_2O_2 above the endogenous capacity of cells to remove it. Consequently, the cell killing was observed [95, 141, 142]. Similar effects were seen in *E. coli* study. The protectiveness of Mn porphyrins towards SOD-deficient *E. coli* was fully reversed in the presence of exogenous ascorbate, due to the increased production of H_2O_2. However, *E. coli* initially ceased to grow, but recovered over time by upregulating endogenous peroxidases and catalases [95]. Such an outcome suggests that in those studies where the anticancer effect of MnP was reported [143], the MnP might have acted in partnership with ascorbate by provoking the cellular adaptive response. Dorai et al. data [144] suggest an adaptive response to the action of MnTnHex-2-PyP^{5+} in a rat warm renal ischemia model also (see below under renal I/R). This action is similar to the upregulation of endogenous antioxidants when the oxidative stress was imposed by physical exercise [145]. A response to enhanced expression of MnSOD and concomitant increase in oxidative stress, by upregulation of some of the peroxide-removing enzymes, was observed by Kim et al. [146].

Reactivity of MnPs toward transcription factors

Several *in vitro* and *in vivo* animal studies show that via removing signaling reactive species MnP inhibits the activation of HIF-1α, AP-1 and that Sp1 with concomitant suppression of oxidative stress [119, 143, 147–149]. In such cases the antioxidative action of MnP exerts antioxidative effects (Figure 10B). The identical ability to accept and donate electrons (as exemplified by identical rates to reduce and oxidize $O_2^{\cdot-}$ [109]) indicates that MnTE-2-PyP^{5+} acts as an equally able pro-oxidant and antioxidant in the dismutation process. Thus, it readily oxidizes ascorbate [142] and cysteine of glutathione in an aqueous system [27]. Further, the data on NF-κB DNA binding in cellular and animal models [150, 151] suggest that cationic Mn porphyrin can approach the deprotonated, anionic cysteines of p50 of NF-κB in nucleus and subsequently oxidize them, which would lead to the suppression of NF-κB activation [151, 152]. In this case, the pro-oxidative action of MnPs translates into antioxidative effects. It is possible that cysteine oxidation by MnP may happen with other transcription factors as well. However, in studies of malignant lymphoma cells that were

treated with glucocorticoids, an oxidative cytosolic event, such as p65 glutationylation by MnP in the presence of H_2O_2, resulted in glutathione deprivation, enhanced oxidative stress and in turn enhanced cancer cell killing [114, 115]. Cases such as these indicate the need to distinguish between the mechanism of action of Mn porphyrins and the nature of the observed effects.

Timing of MnP administration

MnTM-2-PyP^{5+} ameliorates diabetes-induced oxidative stress and affects life-span of diabetic rats when administered for 2 months subcutaneously at 1 mg/kg five times/week followed by a week of rest, starting at the onset of diabetes [160]. MnTM-2-PyP^{5+} treatment suppressed lipid peroxidation and nitrotyrosine formation, prevented aconitase inactivation, and reversed the induction of Na^+/H^+ exchangers [147]. However, when the administration started one week after the onset of diabetes, no protection against oxidative stress and diabetic complications was detected [161]. Moreover, MnTM-2-PyP^{5+} contributed to the kidney damage: increased urinary protein, lysozyme and blood urea nitrogen levels were found. Further, its administration increased malondialdehyde levels and decreased activity of glucose-6-phosphate dehydrogenase. This enzyme has a unique role, as it is a principal source of cellular reducing equivalents in the form of NADPH, which supports glutathione regeneration. In stroke studies, MnTE-2-PyP^{5+} was only efficacious if given not later than 6 hours after middle cerebral artery occlusion (MCAO) [162]. Differences in the effects produced with different dosing regimen are likely related to the changes in the cellular balance between the reactive species and endogenous antioxidants as the disease progresses. Tan et al. recently showed a remarkable ability of MnTnHex-2-PyP^{5+} to reduce the severity of motor deficit in a cerebral palsy model, but only when given to rabbit dam prior to uterine ischemia/reperfusion. The effect was lost if MnP was given during reperfusion, which is due to its slow accumulation in fetal brain (see below under *Cerebral palsy*) [163].

Mn porphyrins and tumors

Numerous reports provide evidence that tumors are more oxidatively stressed than normal tissue [164–177]; moreover, tumors adapt so that they utilize oxidative stress as a "signaling" tool for their own progression. Yet, tumors are also vulnerable to any additional increase in oxidative stress, which may eventually lead to cell apoptosis, exemplified by a narrower bell-shape curve in Figure 12. Data have been provided which show that MnP can suppress tumor progression by either: (1) removal of reactive species as witnessed by the suppression of oxidative stress (see below); or (2) increased production of reactive species (Figure 12). *The type of MnP action depends on cellular redox status, timing of MnP administration, levels of reactive species and MnPs and their co-localization, levels of endogenous antioxidants, and MnP cellular and subcellular distribution.*

A 4T1 breast cancer cellular and mouse studies provide evidence that removal of reactive species by MnTE-2-PyP^{5+} prevents HIF-1α activation and VEGF expression, and thus tumor angiogenesis. Concomitant decrease in oxidative stress was detected [143, 148, 149]. Similarly, in a skin carcinogenesis mouse model, MnP suppressed AP-1 activation and protein oxidative modification [178]. When different cancer cell lines were cultured in the presence of MnP and an excess of ascorbate, the effects observed were pro-oxidative; a similar trend was seen in a 4T1 mouse model [142]. These effects are likely due to the inability of endogenous enzymes to manage excessive H_2O_2 produced by MnP-catalyzed ascorbate oxidation (Figure 11) [142].

Anticancer drugs which function by increasing tumor oxidative burden have been widely used. Prostate cancer cells often exert increased generation of reactive oxygen species from mitochondria [179] or NADPH oxidases [180], which is in part due to the decreased levels

of antioxidant enzymes, such as MnSOD, CuZnSOD, and catalase [181, 182]. Partenolide selectively activates NADPH oxidases, mediating oxidative stress in prostate cancer cells by both increasing ROS generation and decreasing antioxidant defense capacity, which results in radiosensitizing effects. Yet, the oxidative stress in normal prostate epithelial cells was reduced [183].

The *in vivo* and *in vitro* efficacy data

Below are summarized data that show more than 1000-fold increase in the *in vivo* efficacy of lipophilic relative to hydrophilic MnPs, which at least in part reflects their ability to enter the cell and its critical compartments and cross the BBB. Also, a few studies are cited whose data strongly suggest that MnPs can indeed mimic mitochondrial MnSOD.

MnTnHex-2-PyP^{5+} has been studied in several models of central nervous system injuries and has been found efficacious at very low single or multiple doses ranging from 0.05 to 3.2 mg/kg/day in animal models and from 0.1 to 1 μM in *E. coli* studies. The hydrophilic MnTE-2-PyP^{5+} was up to 120-fold less efficacious at 6 to 15 mg/kg single or multiple doses (ip, iv, sc, icv) in animal models, and from ~20 to 50 μM in cellular models [44, 46]. MnTnHex-2-PyP^{5+} was remarkably efficacious in stroke and hemorrhage rodent models [112, 150], rabbit cerebral palsy [163, 191], brain glioma study [192], organotypic hyppocampal slice model of oxygen glucose deprivation [190], rat eye hypertension [193], rat lung radiation [194], rat renal ischemia reperfusion model [144, 195], *E. coli* model [116], and ataxia telangiectasia radiation cellular model [196]. The most remarkable efficacy of MnTnHex-2-PyP^{5+} was found in the rabbit cerebral palsy model (see below under *Cerebral palsy*). Ataxia telangiectasia (AT) is a rare neurodegenerative disease in which the impaired mitochondrial function of lymphoblastoids causes AT patients to be particularly sensitive to radiation. In a cellular model, the 1 μM MnTnHex-2-PyP^{5+} was the most efficacious among a wide range of compounds studied, followed by 56 μM MnTM$_x$-2-PyP^{y+}. MnTM$_x$-2-PyP^{y+} describes a preparation that was incompletely quaternized (methylated) MnT-2-PyP^{+}. It contains Mn porphyrins bearing different number of methyl groups from 0 to 4, and therefore total charge from 1+ to 5+. The preparation was thus more lipophilic relative to a single compound, MnTM-2-PyP^{5+}, bearing 4 methyl groups and a pentacationic charge. $MnCl_2$ was marginally protective, but it was used at only 1 μM concentration. Other compounds studied are: MnSalen derivatives (EUK-8, EUK-134 and EUK-189), Mn cyclic polyamines (M40403, M40304), MnTE-2-PyP^{5+}, PEG-ylated porphyrin, MnTTEG-2-PyP^{5+}, and $MnBr_8TSPP^{3-}$ [196]. The study suggests that positive charge of a compound and its lipophilicity are key features that allow MnTnHex-2-PyP^{5+} to radioprotect mitochondria. In an organotypic hyppocampal slice model of oxygen/glucose deprivation [190], we explored the most lipophilic member of the alkylpyridyl series: the octyl compound, MnTnOct-2-PyP^{5+}. The compound was >1000-fold more efficacious than hydrophilic MnTE-2-PyP^{5+} and its diethylimidazolium analogue, MnTDE-2-ImP^{5+}. In a brain tumor study, MnTnHex-2-PyP^{5+} was an efficacious radio- and chemo-sensitizer. Its efficacy is at least in part due to its ability to cross BBB and accumulate in brain mitochondria [44].

However, lipophilic MnTnHex-2-PyP^{5+} also has micellar characteristics, as it bears cationic polar heads and hydrophobic chains. This contributes at least in part to its increased toxicity. Zn analogue, ZnTnHex-2-PyP^{5+}, exerts no dark toxicity [197], which suggests that redox activity of a metal site contributes to the toxicity of MnTnHex-2-PyP^{5+}. Our efforts were recently directed towards reducing toxicity while maintaining high redox potency and high lipophilicity of MnTnHex-2-PyP^{5+}. Its oxygen derivative, MnTnBuOE-2-PyP^{5+}, was synthesized (Figure 7), and has enhanced $k_{cat}(O_2^{\bullet-})$, lipophilicity and greatly reduced toxicity (Figure 7) [118].

Skin carcinogenesis

In a TPA-skin carcinogenesis model, MnTE-2-PyP^{5+} was administered in a timely manner, after cells underwent apoptosis and before proliferation, and was applied to a mouse skin at 5 ng/day, 5 days per week, for 14 weeks [178]. Mn porphyrin decreased the incidence and multiplicity of papillomas from 31 (in control mice) to 5 (Figure 13). In a similar study with MnSOD-overexpressor mice, MnSOD suppressed both apoptosis and proliferation, and the final outcome was therefore diminished: the number of papillomas decreased from 19 to 9 (Figure 13) [20, 178]. Furthermore, MnTE-2-PyP^{5+} suppressed oxidative stress as shown by the reduced levels of carbonylated proteins. It greatly suppressed AP-1 activation and proliferation and consequently the incidence of cancer, without affecting levels of the pro-apoptotic, tumor suppressor transcription factor p53 (Figure 13). The MnP antioxidative mode of action was proposed as a means to remove signaling reactive species, and thereby spare biological targets and prevent transcriptional activity.

UVB-mediated skin damage

Mitochondrial DNA, mtDNA, is organized as nucleoids in the mitochondrial inner membrane. Nucleoids consist of mtDNA-protein macromolecular complexes containing 2–8 mtDNA molecules associated with various proteins such as mitochondrial transcription factor A, mitochondrial single-strand DNA binding protein and mitochondrial DNA polymerase polyγ protein [198]. Polyγ is the only known polymerase enzyme responsible for the replication and repair of mtDNA. mtDNA is more sensitive to UV-induced damage than is nuclear DNA, as it lacks histones and an elaborate repair system. Depilated mice in resting phase of hair cycle were irradiated with 5 kJ/m^2 of UVB radiation. The oxidative damage of polyγ protein (its nitration and subsequent inactivation [198–200]) was greatly reduced in MnSOD$^{+/+}$ wild type mice as compared to MnSOD knockout mice (Figure 14A). The UVB radiation did not affect levels of polyγ. Such data indicate that MnSOD is a mitochondrial fidelity protein that protects polyγ against UV-induced inactivation. The full protection of polyγ was observed in skin lysates of MnSOD$^{+/-}$ mice, treated twice daily ip for two days before UVB with 5 mg/kg of MnTE-2-PyP^{5+} (Figure 14) [198]. The data provide further evidence that this MnP is indeed a MnSOD mimic.

Pain study – chronic morphine tolerance

Acute morphine has been shown to suppress pain in a mouse paw exposed to heat. When given chronically over 4 days, the analgesic effect was lost but was fully restored if morphine was co-administered with Mn porphyrins (Figure 15) [44]. Chronic morphine tolerance causes MnSOD inactivation but does not affect its expression levels (Figure 15). The oxidative modifications of neurotransmitters, such as glutamate transferase and glutamine synthase, also contribute to the development of chronic morphine tolerance [201, 202]. Both MnTE-2-PyP^{5+} and MnTnHex-2-PyP^{5+} were able to prevent MnSOD inactivation (Figure 15) [201]. The activity of Cu, ZnSOD was affected by neither chronic morphine tolerance nor by MnPs (Figure 15). A lipophilic MnTnHex-2-PyP^{5+} was 30-fold more efficacious, which agrees well with its ability to accumulate 20-fold more in mitochondria than does MnTE-2-PyP^{5+}. As inhibition of chronic morphine tolerance occurs at the level of the central nervous system, the ability of a drug to cross the BBB also plays a role. MnTnHex-2-PyP^{5+} is able to cross the BBB ~9-fold more than MnTE-2-PyP^{5+} [112, 122]. Oxidative stress was suppressed, as seen by the reduction in formation of 8-hydroxy-2′-deoxyguanosine [122].

Renal ischemia-reperfusion

Two sets of data on renal/ischemia have been reported. The first study by Saba et al. provided data on MnSOD inactivation which are similar to the data obtained in a mouse pain

model (Figure 16) [195]. Rats were subjected to a right nephrectomy and renal artery occlusion (40 minutes) followed by 18 hours reperfusion. MnP was given as a single 0.05 mg/kg injection via iv route at 30 minutes and 24 hours before ischemia/reperfusion. The levels of MnSOD were not affected by ischemia/reperfusion, yet MnTnHex-2-PyP^{5+} prevented enzyme inactivation if given 24 hours before the oxidative insult. Further, Mn porphyrin significantly suppressed the protein nitrotyrosine formation in a renal tissue. ATP synthase-β subunit was identified as a key protein induced by MnP and a complex V (ATP synthase) as a target of renal ischemia/reperfusion.

The second study of rat warm renal ischemia by Dorai et al. was conducted with 0.1 mg/kg MnTnHex-2-PyP^{5+}. The MnP was given intramuscularly at 24 hours before, during renal artery clamp and 24 hours after surgery, as a part of a cocktail containing Krebs cycle intermediates, α-ketoglutarate and L-aspartate, and growth factors bFGF, BMP-7, SDF-1 and EPO [144]. At 48 hours, the kidneys were harvested and examined. Significant reversal of morphological changes and a decrease in the specific ischemic markers lipocalin-2, mucin-1 and galectin-3 were detected. Quantitative reverse transcriptase-polymerase chain reaction in treated animals reveal multifold upregulation of several antioxidant genes, including MnSOD and extracellular Cu, ZnSOD.

Cerebral palsy

The role of MnSOD and mitochondria in neurological disorders, such as cerebral palsy and epilepsy, has been established [203, 204]. The predominant pathological lesion underlying cerebral palsy in premature infants is thought to be the result of hypoxic-ischemic injury to the cerebral white matter; the main cell type injured is developing oligodendrocyte, Ol [204]. Overexpression of MnSOD in developing Ols provides protection to mitochondrial membrane potential and reduces cell death in a mild form of cysteine deprivation, indicating glutathione as a primary defect of energy disruption [204]. In a rabbit dam uterus ischemia model, only lipophilic MnTnHex-2-PyP^{5+}, which crosses the BBB to a 9-fold higher level and accumulates 20-fold more in mitochondria than MnTE-2-PyP^{5+} was successful in suppressing symptoms of cerebral palsy [163]. Both compounds were given iv to rabbit dam 30 minutes before and 30 minutes after 40 minute-long uterine ischemia. MnTnHex-2-PyP^{5+} was tested at 0.12 mg/kg and 1.20 mg/kg, and MnTE-2-PyP^{5+} at 15 mg/kg. The lower dose of MnTnHex-2-PyP^{5+} was more efficacious, while the higher dose carried some toxicity. In a control group, 30 kits were stillborn, 38 were hypotonic, and 28 healthy out of 96 fetuses at C-section; in MnTnHex-2-PyP^{5+}-treated groups, 11 kits were stillborn, 10 hypertonic, and 36 normal out of 51 fetuses (no still born kits were found with lower dose of MnTnHex-2-PyP^{5+}). However, when the MnTnHex-2-PyP^{5+} was given only during reperfusion, due to its insufficiently fast accumulation in a fetal brain (as followed by MRI, the t_{max} ~ 2 hours), the effects were small: 20 kits were stillborn, 14 hypertonic, and 8 healthy out of 41 fetuses [163].

Summary

We have described here in details two strategies to bring the redox-active molecule into mitochondria. Both strategies were shown successful in ameliorating mitochondrially-based oxidative stress disorders. The 1st strategy explores the use of true SOD mimics which are able to efficiently catalyze the dismutation of $O_2^{\cdot-}$ and accumulate in mitochondria. Such compounds belong to the class of cationic Mn(III) *N*-substituted pyridyl- and *N*,*N*′–disubstituted imidazolylporphyrins. Some of them have rate constants, k_{cat} ($O_2^{\cdot-}$), nearly identical in magnitude to those of SOD enzymes. Liberman and Skulachev pointed to the preferred accumulation of monocationic phosphonium compounds in mitochondria. Subsequently, Murphy et al pointed to the critical role that lipophilicity plays also. The cationic Mn porphyrin molecule combines in its structure critical features that allow it to

mimic both the action and the site of mitochondrial enzyme, MnSOD: (1) redox active Mn site, (2) multiple cationic charge, and (3) four alkyl chains. The longer the alkyl chains, the higher the Mn porphyrin accumulation in mitochondria. MnTE-2-PyP^{5+} bears fairly short ethyl chains (Figure 2), yet its multiple pentacationic charge compensates for its inferior lipophilicity; in turn this molecule reaches mitochondria where it was shown to mimic MnSOD action in several different models of oxidative stress. The 2nd strategy has been the one employed in the design of MitoQ$_{10}$, where redox-active quinone was linked to monocationic triphenylphosphonium ion and lipophilic alkyl chain in order to enter mitochondria. As a consequence of such elegant design, numerous Mito-derivatized redox modulators, able to reduce levels of a variety of reactive species (H_2O_2, NO, $ONOO^-$, lipid peroxyl and alkoxyl radicals, etc) which are involved in mitochondrial dysfunction, have been reported: MitoSOX™ Red, MitoSNO, MitoSalen, Mito-Nitroxides (Mito-Tempol, Mito-CP and Mito-CTP), MitoEbselen, MitoB, Mito-αToc. Among those compounds, MitoSOX™ Red bears dihydroethidium as a redox-active unit, which reacts stoichiometrically with $O_2^{\cdot -}$, and is thus often used as a mechanistic tool to provide evidence that $O_2^{\cdot -}$ has indeed been involved in a mitochondrially-based disorder. Caution needs to be exercised because modulatory effect of MitoSOX™ Red (but not SOX – dihydroethydium- in its own right) on cellular bioenergetics has recently been observed [103]. Other compounds, which were shown beneficial in reducing oxidative stress, and for which some evidence exists that they reach mitochondria, have also been discussed.

Acknowledgments

We acknowledge the support of IBH general research funds Duke University's CTSA grant 1 UL 1 RR024128-01 from NCRR/NIH (AT, IBH, IS), W.H. Coulter Translational Partners Grant Program (IBH, AT and IS), NIH U19AI067798 (ZV, IBH and AT), R01 DA024074 (DS and IBH), and RO1 CA 139843 (SM and DKS). IS thanks NIH/NCI Duke Comprehensive Cancer Center Core Grant (5-P30-CA14236-29). Authors are thankful to Irwin Fridovich for critical reading.

Abbreviations

AP-1	activator protein-1
bFGF	basic fibroblast growth factor
BMP-7	bone morphogenic protein-7
$CO_3^{\bullet -}$	carbonate radical
DMBA	7,12-dimethylbenz (*a*)-anthracene
$E_{1/2}$	half-wave reduction potential
EPO	erythropoietin
HClO	hypochlorous acid
HIF-1α	hypoxia inducible factor-1α
icv	intracerebroventricular
IL-1	interleukin-1
IL-6	interleukin-6
ip	intraperitoneal
iv	intravenous
NF-κB	nuclear factor κB
NHE	normal hydrogen electrode

$^{\cdot}OH$	hydroxyl radical
$O_2^{\bullet-}$	superoxide
$ONOO^-$	peroxynitrite
P_{OW}	partition between n-octanol and water
R_f	thin-layer chromatographic retention factor that presents the ratio between the solvent and compound path in 1:1:8=$KNO_{3(sat)}$:H_2O:CH_3CN solvent system
$RO_2^{\cdot}$ ($RO^{\cdot}$)	lipid peroxyl (alkoxyl) radicals
ROS	reactive oxygen species
RS	reactive species
SAR	structure-activity relationship
sc	subcutaneous
SDF-1	stromal cell derived factor-1
SOD	superoxide dismutase
Sp1	specificity protein 1
TPA	12-*O*-tetradecanoylphorbol-13-acetate
UQ/UQH$^{\cdot}$	ubiquinone/ubisemiquinone
VEGF	vascular endothelial growth factor; charges in the MnP abbreviations are omitted throughout Figure legends
MnPs	Mn(III) *N*-alkylpyridylporphyrins
$Mn^{III}P$ to $Mn^{II}P$	oxidized (Mn +3 oxidation state) and reduced Mn porphyrin (Mn +2 oxidation state), total charge 5+ and 4+ are omitted in text
BBB	blood brain barrier
$MnTPP^+$	Mn(III) *meso*-tetrakisphenylporphyrin
$MnTM\text{-}2\text{-}PyP^{5+}$	Mn(III) *meso*-tetrakis(*N*-methylpyridinum-2-yl)porphyrin
$MnT\text{-}2\text{-}PyP^+$	Mn(III) *meso-tetrakis* (*N*-pyridinium-2-yl)porphyrin
$MnTE\text{-}2\text{-}PyP^{5+}$	AEOL10113, FBC-007, Mn(III) *meso*-tetrakis(*N*-ethylpyridinum-2-yl)porphyrin
$MnTnHex\text{-}2\text{-}PyP^{5+}$	Mn(III) *meso*-tetrakis(*N*-n-hexylpyridinum-2-yl)porphyrin
$MnTnHex\text{-}3\text{-}PyP^{5+}$	Mn(III) *meso*-tetrakis(*N*-n-hexylpyridinum-3-yl)porphyrin
$MnTnOct\text{-}2\text{-}PyP^{5+}$	Mn(III) *meso*-tetrakis(*N*-n-octylpyridinum-2-yl)porphyrin
$MnBr_8TM\text{-}3\text{-}PyP^{4+}$	Mn(II) β-octabromo-*meso*-tetrakis(*N*-methylpyridinum-3-yl)porphyrin

$MnCl_5TE\text{-}2\text{-}PyP^{4+}$	Mn(II) β-pentachloro-*meso*-tetrakis(*N*-ethylpyridinum-2-yl)porphyrin
$MnTMOHex\text{-}3\text{-}PyP^{5+}$	Mn(III) *meso*-tetrakis(*N*-(6′-methoxyhexyl)pyridinum-3-yl)porphyrin
$MnTnBuOE\text{-}2\text{-}PyP^{5+}$ (BMX-001)	Mn(III) *meso*-tetrakis*(N*-2′-butoxyethylpyridinium-2-yl)porphyrin
$MnTDE\text{-}2\text{-}ImP^{5+}$ (AEOL10150)	Mn(III) *meso*-tetrakis(*N*, *N*′-diethylimidazolium-2-yl)porphyrin
$MnMImP_3P^{2+}$	Mn(III) 5,10,15-trisimidazolium-20-mono(*N*, *N*′-dimethylimidazolium-2-yl)porphyrin
$MnTBAP^{3-}$ (also $MnTCPP^{3-}$ and AEOL10201)	Mn(III) *meso*-tetrakis(4-carboxylatophenyl)porphyrin
$MnTM\text{-}4\text{-}PyP^{5+}$	manganese(III) *meso*-tetrakis(*N*-methylpyridinium-4-yl)porphyrin
MnTECP	manganese *meso*-tetrakis-(ethoxycarbonyl) porphyrin
$FeTE\text{-}2\text{-}PyP(OH)^{4+}$	Fe(III) monohydroxo *meso*-tetrakis(*N*-ethylpyridinum-2-yl)porphyrin

References

1. Forman HJ, Maiorino M, Ursini F. Signaling functions of reactive oxygen species. Biochemistry. 2010; 49:835–842. [PubMed: 20050630]
2. Christianson DW. Structural chemistry and biology of manganese metalloenzymes. Prog Biophys Mol Biol. 1997; 67:217–252. [PubMed: 9446936]
3. Church SL, Grant JW, Ridnour LA, Oberley LW, Swanson PE, Meltzer PS, Trent JM. Increased manganese superoxide dismutase expression suppresses the malignant phenotype of human melanoma cells. Proc Natl Acad Sci USA. 1993; 90:3113–3117. [PubMed: 8464931]
4. Li JJ, Oberley LW, St Clair DK, Ridnour LA, Oberley TD. Phenotypic changes induced in human breast cancer cells by overexpression of manganese-containing superoxide dismutase. Oncogene. 1995; 10:1989–2000. [PubMed: 7761099]
5. Van Remmen H, Ikeno Y, Hamilton M, Pahlavani M, Wolf N, Thorpe SR, Alderson NL, Baynes JW, Epstein CJ, Huang TT, Nelson J, Strong R, Richardson A. Life-long reduction in MnSOD activity results in increased DNA damage and higher incidence of cancer but does not accelerate aging. Physiol Genomics. 2003; 16:29–37. [PubMed: 14679299]
6. Zhong W, Oberley LW, Oberley TD, St Clair DK. Suppression of the malignant phenotype of human glioma cells by overexpression of manganese superoxide dismutase. Oncogene. 1997; 14:481–490. [PubMed: 9053845]
7. Gregory EM, Fridovich I. Oxygen toxicity and the superoxide dismutase. J Bacteriol. 1973; 114:1193–1197. [PubMed: 4197269]
8. Saltzman HA, Fridovich I. Editorial: Oxygen toxicity. Introduction to a protective enzyme: superoxide dismutase. Circulation. 1973; 48:921–923. [PubMed: 4584616]
9. Ravindranath SD, Fridovich I. Isolation and characterization of a manganese-containing superoxide dismutase from yeast. J Biol Chem. 1975; 250:6107–6112. [PubMed: 238997]
10. Gabbianelli R, Battistoni A, Polizio F, Carri MT, De Martino A, Meier B, Desideri A, Rotilio G. Metal uptake of recombinant cambialistic superoxide dismutase from Propionibacterium shermanii is affected by growth conditions of host Escherichia coli cells. Bioiochem, Biophys Res Commun. 1995; 216:841–847.

11. Lebovitz RM, Zhang H, Vogel H, Cartwright J Jr, Dionne L, Lu N, Huang S, Matzuk MM. Neurodegeneration, myocardial injury, and perinatal death in mitochondrial superoxide dismutase-deficient mice. Proc Natl Acad Sci USA. 1996; 93:9782–9787. [PubMed: 8790408]
12. Li Y, Huang TT, Carlson EJ, Melov S, Ursell PC, Olson JL, Noble LJ, Yoshimura MP, Berger C, Chan PH, Wallace DC, Epstein CJ. Dilated cardiomyopathy and neonatal lethality in mutant mice lacking manganese superoxide dismutase. Nat Genet. 1995; 11:376–381. [PubMed: 7493016]
13. Holley AK, Dhar SK, Xu Y, St Clair DK. Manganese superoxide dismutase: beyond life and death. Amino acids. 2010
14. Miriyala S, Holley AK, St Clair DK. Mitochondrial superoxide dismutase--signals of distinction. Anti-cancer Agents Med Chem. 2011; 11:181–190.
15. Buettner GR. Superoxide dismutase in redox biology: the roles of superoxide and hydrogen peroxide. Anti-cancer Agents Med Chem. 2011; 11:341–346.
16. Buettner GR, Ng CF, Wang M, Rodgers VG, Schafer FQ. A new paradigm: manganese superoxide dismutase influences the production of H2O2 in cells and thereby their biological state. Free Radic Biol Med. 2006; 41:1338–1350. [PubMed: 17015180]
17. Li S, Yan T, Yang JQ, Oberley TD, Oberley LW. The role of cellular glutathione peroxidase redox regulation in the suppression of tumor cell growth by manganese superoxide dismutase. Cancer Res. 2000; 60:3927–3939. [PubMed: 10919671]
18. Wang M, Kirk JS, Venkataraman S, Domann FE, Zhang HJ, Schafer FQ, Flanagan SW, Weydert CJ, Spitz DR, Buettner GR, Oberley LW. Manganese superoxide dismutase suppresses hypoxic induction of hypoxia-inducible factor-1alpha and vascular endothelial growth factor. Oncogene. 2005; 24:8154–8166. [PubMed: 16170370]
19. Hempel N, Carrico PM, Melendez JA. Manganese superoxide dismutase (Sod2) and redox-control of signaling events that drive metastasis. Anti-cancer Agents Med Chem. 2011; 11:191–201.
20. Zhao Y, Xue Y, Oberley TD, Kiningham KK, Lin SM, Yen HC, Majima H, Hines J, St Clair D. Overexpression of manganese superoxide dismutase suppresses tumor formation by modulation of activator protein-1 signaling in a multistage skin carcinogenesis model. Cancer Res. 2001; 61:6082–6088. [PubMed: 11507057]
21. Behrend L, Mohr A, Dick T, Zwacka RM. Manganese superoxide dismutase induces p53-dependent senescence in colorectal cancer cells. Mol Cell Biol. 2005; 25:7758–7769. [PubMed: 16107721]
22. Chandhok NS, Pellman D. A little CIN may cost a lot: revisiting aneuploidy and cancer. Curr Opin Genet Dev. 2009; 19:74–81. [PubMed: 19195877]
23. Ganem NJ, Storchova Z, Pellman D. Tetraploidy, aneuploidy and cancer. Curr Opin Genet Dev. 2007; 17:157–162. [PubMed: 17324569]
24. Mesquita A, Weinberger M, Silva A, Sampaio-Marques B, Almeida B, Leao C, Costa V, Rodrigues F, Burhans WC, Ludovico P. Caloric restriction or catalase inactivation extends yeast chronological lifespan by inducing H2O2 and superoxide dismutase activity. Proc Natl Acad Sci USA. 2010; 107:15123–15128. [PubMed: 20696905]
25. Oberley LW, Buettner GR. Role of superoxide dismutase in cancer: a review. Cancer Res. 1979; 39:1141–1149. [PubMed: 217531]
26. Oberley LW, Oberley TD, Buettner GR. Cell differentiation, aging and cancer: the possible roles of superoxide and superoxide dismutases. Med Hypotheses. 1980; 6:249–268. [PubMed: 6253771]
27. Batinic-Haberle I, Spasojevic I, Tse HM, Tovmasyan A, Rajic Z, St Clair DK, Vujaskovic Z, Dewhirst MW, Piganelli JD. Design of Mn porphyrins for treating oxidative stress injuries and their redox-based regulation of cellular transcriptional activities. Amino acids. 2010
28. Fridovich I. Superoxide dismutases: anti- versus pro- oxidants? Anti-cancer Agents Med Chem. 2011; 11:175–177.
29. MacMillan-Crow LA, Crow JP. Does more MnSOD mean more hydrogen peroxide? Anti-cancer Agents Med Chem. 2011; 11:178–180.
30. Szlosarek P, Charles KA, Balkwill FR. Tumour necrosis factor-alpha as a tumour promoter. Eur J Cancer. 2006; 42:745–750. [PubMed: 16517151]
31. Kwei KA, Finch JS, Thompson EJ, Bowden GT. Transcriptional repression of catalase in mouse skin tumor progression. Neoplasia. 2004; 6:440–448. [PubMed: 15548352]

32. Gao MC, Jia XD, Wu QF, Cheng Y, Chen FR, Zhang J. Silencing Prx1 and/or Prx5 sensitizes human esophageal cancer cells to ionizing radiation and increases apoptosis via intracellular ROS accumulation. Acta Pharmacol Sin. 2011; 32:528–536. [PubMed: 21468086]
33. Sampson N, Koziel R, Zenzmaier C, Bubendorf L, Plas E, Jansen-Durr P, Berger P. ROS signaling by NOX4 drives fibroblast-to-myofibroblast differentiation in the diseased prostatic stroma. Mol Endocrinol. 2011; 25:503–515. [PubMed: 21273445]
34. Shen KK, Ji LL, Chen Y, Yu QM, Wang ZT. Influence of glutathione levels and activity of glutathione-related enzymes in the brains of tumor-bearing mice. Biosci Trends. 2011; 5:30–37. [PubMed: 21422598]
35. Sorokina LV, Solyanik GI, Pyatchanina TV. The evaluation of prooxidant and antioxidant state of two variants of lewis lung carcinoma: a comparative study. Exp Oncol. 2010; 32:249–253. [PubMed: 21270753]
36. Nonn L, Berggren M, Powis G. Increased expression of mitochondrial peroxiredoxin-3 (thioredoxin peroxidase-2) protects cancer cells against hypoxia and drug-induced hydrogen peroxide-dependent apoptosis. Mol Can Res: MCR. 2003; 1:682–689.
37. Glorieux C, Dejeans N, Sid B, Beck R, Calderon PB, Verrax J. Catalase overexpression in mammary cancer cells leads to a less aggressive phenotype and an altered response to chemotherapy. Biochem Pharmacol. 2011
38. Dhar SK, Tangpong J, Chaiswing L, Oberley TD, St Clair DK. Manganese superoxide dismutase is a p53-regulated gene that switches cancers between early and advanced stages. Cancer Res. 2011; 71:6684–6695. [PubMed: 22009531]
39. Bartesaghi S, Wenzel J, Trujillo M, Lopez M, Joseph J, Kalyanaraman B, Radi R. Lipid peroxyl radicals mediate tyrosine dimerization and nitration in membranes. Chem Res Toxicol. 2010; 23:821–835. [PubMed: 20170094]
40. Moreno DM, Marti MA, De Biase PM, Estrin DA, Demicheli V, Radi R, Boechi L. Exploring the molecular basis of human manganese superoxide dismutase inactivation mediated by tyrosine 34 nitration. Arch Biochem Biophys. 2011; 507:304–309. [PubMed: 21167124]
41. Shan W, Zhong W, Zhao R, Oberley TD. Thioredoxin 1 as a subcellular biomarker of redox imbalance in human prostate cancer progression. Free radical biology & medicine. 2010; 49:2078–2087. [PubMed: 20955789]
42. Pasternack RF, Halliwell B. Superoxide dismutase activities of an iron porphyrin and other iron complexes. J Am Chem Soc. 1979; 101:1026–1031.
43. Batinic-Haberle I. SOD enzymes and their mimics in cancer: pro vs anti-odixative mode of action-part II. Anti-cancer Agents Med Chem. 2011; 11:327–328.
44. Batinic-Haberle I, Rajic Z, Tovmasyan A, Reboucas JS, Ye X, Leong KW, Dewhirst MW, Vujaskovic Z, Benov L, Spasojevic I. Diverse functions of cationic Mn(III) N-substituted pyridylporphyrins, recognized as SOD mimics. Free Radic Biol Med. 2011; 51:1035–1053. [PubMed: 21616142]
45. Batinic-Haberle, I.; Reboucas, JS.; Benov, L.; Spasojevic, I. Chemistry, biology and medical effects of water soluble metalloporphyrins. In: Kadish, KM.; Smith, KM.; Guillard, R., editors. Handbook of Porphyrin Science. Vol. 11. World Scientific; Singapore: 2011. p. 291-393.
46. Batinic-Haberle I, Reboucas JS, Spasojevic I. Superoxide dismutase mimics: chemistry, pharmacology, and therapeutic potential. Antioxid Redox Signal. 2010; 13:877–918. [PubMed: 20095865]
47. Archibald FS, Fridovich I. Manganese, superoxide dismutase, and oxygen tolerance in some lactic acid bacteria. J Bacteriol. 1981; 146:928–936. [PubMed: 6263860]
48. Archibald FS, Fridovich I. The scavenging of superoxide radical by manganous complexes: in vitro. Arch Biochem Biophys. 1982; 214:452–463. [PubMed: 6284026]
49. Barnese K, Gralla EB, Cabelli DE, Valentine JS. Manganous phosphate acts as a superoxide dismutase. J Am Chem Soc. 2008; 130:4604–4606. [PubMed: 18341341]
50. Culotta VC, Yang M, Hall MD. Manganese transport and trafficking: lessons learned from Saccharomyces cerevisiae. Eukaryot Cell. 2005; 4:1159–1165. [PubMed: 16002642]

51. Liberman EA, Topaly VP, Tsofina LM, Jasaitis AA, Skulachev VP. Mechanism of coupling of oxidative phosphorylation and the membrane potential of mitochondria. Nature. 1969; 222:1076–1078. [PubMed: 5787094]
52. Murphy MP. Targeting lipophilic cations to mitochondria. Biochim Biophys Acta. 2008; 1777:1028–1031. [PubMed: 18439417]
53. Murphy MP, Smith RA. Targeting antioxidants to mitochondria by conjugation to lipophilic cations. Annu Rev Pharmacol Toxicol. 2007; 47:629–656. [PubMed: 17014364]
54. Mahammed A, Gross Z. Highly efficient catalase activity of metallocorroles. Chem Commun (Camb). 2010; 46:7040–7042. [PubMed: 20730224]
55. Epperly MW, Tyurina YY, Nie S, Niu YY, Zhang X, Kagan V, Greenberger JS. MnSOD-plasmid liposome gene therapy decreases ionizing irradiation-induced lipid peroxidation of the esophagus. In Vivo. 2005; 19:997–1004. [PubMed: 16277013]
56. Asayama S, Kawamura E, Nagaoka S, Kawakami H. Design of manganese porphyrin modified with mitochondrial signal peptide for a new antioxidant. Mol Pharmaceut. 2006; 3:468–470.
57. He K, Nukada H, Urakami T, Murphy MP. Antioxidant and pro-oxidant properties of pyrroloquinoline quinone (PQQ): implications for its function in biological systems. Biochem Pharmacol. 2003; 65:67–74. [PubMed: 12473380]
58. Misra HS, Khairnar NP, Barik A, Indira Priyadarsini K, Mohan H, Apte SK. Pyrroloquinoline-quinone: a reactive oxygen species scavenger in bacteria. FEBS Lett. 2004; 578:26–30. [PubMed: 15581610]
59. Bishop A, Gallop PM, Karnovsky ML. Pyrroloquinoline quinone: a novel vitamin? Nutr Rev. 1998; 56:287–293. [PubMed: 9810806]
60. Jensen FE, Gardner GJ, Williams AP, Gallop PM, Aizenman E, Rosenberg PA. The putative essential nutrient pyrroloquinoline quinone is neuroprotective in a rodent model of hypoxic/ischemic brain injury. Neuroscience. 1994; 62:399–406. [PubMed: 7830887]
61. Smidt CR, Steinberg FM, Rucker RB. Physiologic importance of pyrroloquinoline quinone. Proc Soc Exp Biol Med. 1991; 197:19–26. [PubMed: 1850521]
62. Zhang Y, Feustel PJ, Kimelberg HK. Neuroprotection by pyrroloquinoline quinone (PQQ) in reversible middle cerebral artery occlusion in the adult rat. Brain Res. 2006; 1094:200–206. [PubMed: 16709402]
63. Zhang Y, Rosenberg PA. The essential nutrient pyrroloquinoline quinone may act as a neuroprotectant by suppressing peroxynitrite formation. Eur J Neurosci. 2002; 16:1015–1024. [PubMed: 12383230]
64. Zhu BQ, Simonis U, Cecchini G, Zhou HZ, Li L, Teerlink JR, Karliner JS. Comparison of pyrroloquinoline quinone and/or metoprolol on myocardial infarct size and mitochondrial damage in a rat model of ischemia/reperfusion injury. J Cardiovasc Pharmacol Ther. 2006; 11:119–128. [PubMed: 16891289]
65. Zhu BQ, Zhou HZ, Teerlink JR, Karliner JS. Pyrroloquinoline quinone (PQQ) decreases myocardial infarct size and improves cardiac function in rat models of ischemia and ischemia/reperfusion. Cardiovasc Drugs Ther. 2004; 18:421–431. [PubMed: 15770429]
66. Giles SS, Batinic-Haberle I, Perfect JR, Cox GM. Cryptococcus neoformans mitochondrial superoxide dismutase: an essential link between antioxidant function and high-temperature growth. Eukaryot Cell. 2005; 4:46–54. [PubMed: 15643059]
67. Spasojevic I, Batinic-Haberle I, Stevens RD, Hambright P, Thorpe AN, Grodkowski J, Neta P, Fridovich I. Manganese(III) biliverdin IX dimethyl ester: a powerful catalytic scavenger of superoxide employing the Mn(III)/Mn(IV) redox couple. Inorg Chem. 2001; 40:726–739. [PubMed: 11225116]
68. Reboucas JS, Spasojevic I, Batinic-Haberle I. Pure manganese(III) 5,10,15,20-tetrakis(4-benzoic acid)porphyrin (MnTBAP) is not a superoxide dismutase mimic in aqueous systems: a case of structure-activity relationship as a watchdog mechanism in experimental therapeutics and biology. J Biol Inorg Chem. 2008; 13:289–302. [PubMed: 18046586]
69. Vorotnikova E, Rosenthal RA, Tries M, Doctrow SR, Braunhut SJ. Novel synthetic SOD/catalase mimetics can mitigate capillary endothelial cell apoptosis caused by ionizing radiation. Rad Res. 2010; 173:748–759.

70. Keaney M, Matthijssens F, Sharpe M, Vanfleteren J, Gems D. Superoxide dismutase mimetics elevate superoxide dismutase activity in vivo but do not retard aging in the nematode Caenorhabditis elegans. Free Radic Biol Med. 2004; 37:239–250. [PubMed: 15203195]
71. Melov S, Doctrow SR, Schneider JA, Haberson J, Patel M, Coskun PE, Huffman K, Wallace DC, Malfroy B. Lifespan extension and rescue of spongiform encephalopathy in superoxide dismutase 2 nullizygous mice treated with superoxide dismutase-catalase mimetics. J Neurosci. 2001; 21:8348–8353. [PubMed: 11606622]
72. Haruyama T, Asayama S, Kawakami H. Highly amphiphilic manganese porphyrin for the mitochondrial targeting antioxidant. J Biochem. 2010; 147:153–156. [PubMed: 19880373]
73. Trnka J, Blaikie FH, Logan A, Smith RA, Murphy MP. Antioxidant properties of MitoTEMPOL and its hydroxylamine. Free Radic Res. 2009; 43:4–12. [PubMed: 19058062]
74. Floyd RA, Chandru HK, He T, Towner R. Anti-cancer activity of nitrones and observations on mechanism of action. Anti-cancer Agents Med Chem. 2011; 11:373–379.
75. Floyd RA. Hydroxyl free-radical spin-adduct in rat brain synaptosomes. Observations on the reduction of the nitroxide. Biochim Biophys Acta. 1983; 756:204–216. [PubMed: 6299374]
76. Alexandre J, Nicco C, Chereau C, Laurent A, Weill B, Goldwasser F, Batteux F. Improvement of the therapeutic index of anticancer drugs by the superoxide dismutase mimic mangafodipir. J Natl Cancer Inst. 2006; 98:236–244. [PubMed: 16478742]
77. Bedda S, Laurent A, Conti F, Chereau C, Tran A, Tran-Van Nhieu J, Jaffray P, Soubrane O, Goulvestre C, Calmus Y, Weill B, Batteux F. Mangafodipir prevents liver injury induced by acetaminophen in the mouse. J Hepatol. 2003; 39:765–772. [PubMed: 14568259]
78. Szeto HH, Schiller PW. Novel Therapies targeting inner mitochondrial membrane-from discovery to clinical development. Pharm Res. 2011
79. Yang L, Zhao K, Calingasan NY, Luo G, Szeto HH, Beal MF. Mitochondria targeted peptides protect against 1-methyl-4-phenyl-1,2,3,6-tetrahydropyridine neurotoxicity. Antioxid Redox Signal. 2009; 11:2095–2104. [PubMed: 19203217]
80. Halliwell, B.; Gutteridge, JMC. Free Radicals in Biology and Medicine. Oxford University Press; New York: 2007.
81. Cho S, Szeto HH, Kim E, Kim H, Tolhurst AT, Pinto JT. A novel cell-permeable antioxidant peptide, SS31, attenuates ischemic brain injury by down-regulating CD36. J Biol Chem. 2007; 282:4634–4642. [PubMed: 17178711]
82. Reboucas JS, DeFreitas-Silva G, Spasojevic I, Idemori YM, Benov L, Batinic-Haberle I. Impact of electrostatics in redox modulation of oxidative stress by Mn porphyrins: protection of SOD-deficient Escherichia coli via alternative mechanism where Mn porphyrin acts as a Mn carrier. Free Radic Biol Med. 2008; 45:201–210. [PubMed: 18457677]
83. de Duve C. The origin of eukaryotes: a reappraisal. Nat Rev Genet. 2007; 8:395–403. [PubMed: 17429433]
84. Al-Maghrebi M, Fridovich I, Benov L. Manganese supplementation relieves the phenotypic deficits seen in superoxide-dismutase-null Escherichia coli. Arch Biochem Biophys. 2002; 402:104–109. [PubMed: 12051688]
85. Reddi AR, Jensen LT, Naranuntarat A, Rosenfeld L, Leung E, Shah R, Culotta VC. The overlapping roles of manganese and Cu/Zn SOD in oxidative stress protection. Free Radic Biol Med. 2009; 46:154–162. [PubMed: 18973803]
86. Sanchez RJ, Srinivasan C, Munroe WH, Wallace MA, Martins J, Kao TY, Le K, Gralla EB, Valentine JS. Exogenous manganous ion at millimolar levels rescues all known dioxygen-sensitive phenotypes of yeast lacking CuZnSOD. J Biol Inorg Chem. 2005; 10:913–923. [PubMed: 16283393]
87. Lin YT, Hoang H, Hsieh SI, Rangel N, Foster AL, Sampayo JN, Lithgow GJ, Srinivasan C. Manganous ion supplementation accelerates wild type development, enhances stress resistance, and rescues the life span of a short-lived Caenorhabditis elegans mutant. Free Radic Biol Med. 2006; 40:1185–1193. [PubMed: 16545686]
88. Rosenthal RA, Huffman KD, Fisette LW, Damphousse CA, Callaway WB, Malfroy B, Doctrow SR. Orally available Mn porphyrins with superoxide dismutase and catalase activities. J Biol Inorg Chem. 2009; 14:979–991. [PubMed: 19504132]

89. James AM, Cocheme HM, Smith RA, Murphy MP. Interactions of mitochondria-targeted and untargeted ubiquinones with the mitochondrial respiratory chain and reactive oxygen species. Implications for the use of exogenous ubiquinones as therapies and experimental tools. J Biol Chem. 2005; 280:21295–21312. [PubMed: 15788391]

90. Goldstein S, Czapski G, Heller A. Osmium tetroxide, used in the treatment of arthritic joints, is a fast mimic of superoxide dismutase. Free Radic Biol Med. 2005; 38:839–845. [PubMed: 15749379]

91. Kos I, Reboucas JS, DeFreitas-Silva G, Salvemini D, Vujaskovic Z, Dewhirst MW, Spasojevic I, Batinic-Haberle I. Lipophilicity of potent porphyrin-based antioxidants: comparison of ortho and meta isomers of Mn(III) N-alkylpyridylporphyrins. Free Radic Biol Med. 2009; 47:72–78. [PubMed: 19361553]

92. Engelmann FM, Rocha SV, Toma HE, Araki K, Baptista MS. Determination of n-octanol/water partition and membrane binding of cationic porphyrins. Int J Pharm. 2007; 329:12–18. [PubMed: 16979860]

93. Ross MF, Prime TA, Abakumova I, James AM, Porteous CM, Smith RA, Murphy MP. Rapid and extensive uptake and activation of hydrophobic triphenylphosphonium cations within cells. Biochem J. 2008; 411:633–645. [PubMed: 18294140]

94. Maroz A, Anderson RF, Smith RA, Murphy MP. Reactivity of ubiquinone and ubiquinol with superoxide and the hydroperoxyl radical: implications for in vivo antioxidant activity. Free Radic Biol Med. 2009; 46:105–109. [PubMed: 18977291]

95. Batinic-Haberle I, Rajic Z, Benov L. A combination of two antioxidants (an SOD mimic and ascorbate) produces a pro-oxidative effect forcing Escherichia coli to adapt via induction of oxyR regulon. Anti-cancer Agents Med Chem. 2011; 11:329–340.

96. Kelso GF, Porteous CM, Coulter CV, Hughes G, Porteous WK, Ledgerwood EC, Smith RA, Murphy MP. Selective targeting of a redox-active ubiquinone to mitochondria within cells: antioxidant and antiapoptotic properties. J Biol Chem. 2001; 276:4588–4596. [PubMed: 11092892]

97. Kalyanaraman B. Oxidative chemistry of fluorescent dyes: implications in the detection of reactive oxygen and nitrogen species. Biochem Soc Trans. 2011; 39:1221–1225. [PubMed: 21936793]

98. Cheng G, Lopez M, Zielonka J, Hauser AD, Joseph J, McAllister D, Rowe JJ, Sugg SL, Williams CL, Kalyanaraman B. Mitochondria-targeted nitroxides exacerbate Fluvastatin-mediated cytostatic and cytotoxic effects in breast cancer cells. Cancer Biol Ther. 2011; 12

99. Dessolin J, Schuler M, Quinart A, De Giorgi F, Ghosez L, Ichas F. Selective targeting of synthetic antioxidants to mitochondria: towards a mitochondrial medicine for neurodegenerative diseases? Eur J Pharmacol. 2002; 447:155–161. [PubMed: 12151007]

100. Chouchani ET, Hurd TR, Nadtochiy SM, Brookes PS, Fearnley IM, Lilley KS, Smith RA, Murphy MP. Identification of S-nitrosated mitochondrial proteins by S-nitrosothiol difference in gel electrophoresis (SNO-DIGE): implications for the regulation of mitochondrial function by reversible S-nitrosation. Biochem J. 2010; 430:49–59. [PubMed: 20533907]

101. Cocheme HM, Quin C, McQuaker SJ, Cabreiro F, Logan A, Prime TA, Abakumova I, Patel JV, Fearnley IM, James AM, Porteous CM, Smith RA, Saeed S, Carre JE, Singer M, Gems D, Hartley RC, Partridge L, Murphy MP. Measurement of H2O2 within living Drosophila during aging using a ratiometric mass spectrometry probe targeted to the mitochondrial matrix. Cell Metab. 2011; 13:340–350. [PubMed: 21356523]

102. Aird KM, Allensworth JL, Batinic-Haberle I, Lyerly HK, Dewhirst MW, Devi GR. ErbB1/2 tyrosine kinase inhibitor mediates oxidative stress-induced apoptosis in inflammatory breast cancer cells. Breast Cancer Res Treat. 2011

103. Cheng G, Zielonka J, Kalyanaraman B. Modulatory effects of MitoSOX on cellular bioenergetics: a cautionary note. Free Radic Biol Med. 2011; 51:S37.

104. Smith RA, Murphy MP. Animal and human studies with the mitochondria-targeted antioxidant MitoQ. Ann N Y Acad Sci. 2010; 1201:96–103. [PubMed: 20649545]

105. Ellerby LM, Cabelli DE, Graden JA, Valentine JS. Copper zinc superoxide dismutase: why not pH-dependent? J Am Chem Soc. 1996; 118:6556–6561.

106. Klug-Roth D, Fridovich I, Rabani J. Pulse radiolytic investigations of superoxide catalyzed disproportionation. Mechanism for bovine superoxide dismutase. J Am Chem Soc. 1973; 95:2786–2790. [PubMed: 4632912]

107. Vance CK, Miller AF. A simple proposal that can explain the inactivity of metal-substituted superoxide dismutases. J Am Chem Soc. 1998; 120:461–467.

108. Spasojevic I, Batinic-Haberle I, Reboucas JS, Idemori YM, Fridovich I. Electrostatic contribution in the catalysis of O2*-dismutation by superoxide dismutase mimics. MnIIITE-2-PyP5+ versus MnIIIBr8T-2-PyP+ Biol Chem. 2003; 278:6831–6837.

109. Batinic-Haberle I, Spasojevic I, Stevens RD, Hambright P, Neta P, Okado-Matsumoto A, Fridovich I. New class of potent catalysts of O2.-dismutation. Mn(III) ortho-methoxyethylpyridyl- and di-ortho-methoxyethylimidazolylporphyrins. Dalton Trans. 2004:1696–1702. [PubMed: 15252564]

110. Batinic-Haberle I, Benov L, Spasojevic I, Hambright P, Crumbliss AL, Fridovich I. The relationship between redox potentials, proton dissociation constants of pyrrolic nitrogens, and in vitro and in vivo superoxide dismutase activities of manganese(III) and iron(III) cationic and anionic porphyrins. Inorg Chem. 1999; 38:4011–4022.

111. Abreu IA, Cabelli DE. Superoxide dismutases-a review of the metal-associated mechanistic variations. Biochim Biophys Acta. 2010; 1804:263–274. [PubMed: 19914406]

112. Sheng H, Spasojevic I, Tse HM, Jung JY, Hong J, Zhang Z, Piganelli JD, Batinic-Haberle I, Warner DS. Neuroprotective eEfficacy from a lipophilic redox-modulating Mn(III) *N*-hexylpyridylporphyrin, MnTnHex-2-PyP: rodent models of ischemic stroke and subarachnoid hemorrhage. J Pharmacol Exp Ther. 2011; 338:906–916. [PubMed: 21652782]

113. Ross AD, Sheng H, Warner DS, Piantadosi CA, Batinic-Haberle I, Day BJ, Crapo JD. Hemodynamic effects of metalloporphyrin catalytic antioxidants: structure-activity relationships and species specificity. Free Radic Biol Med. 2002; 33:1657–1669. [PubMed: 12488134]

114. Jaramillo MC, Briehl MM, Tome ME. Manganese porphyrin glutathionylates the p65 subunit of NF-κB to potentiate glucocorticoid-induced apoptosis in lymphoma. Free Radic Biol Med. 2010; 49:S63.

115. Jaramillo MC, Frye JB, Crapo JD, Briehl MM, Tome ME. Increased manganese superoxide dismutase expression or treatment with manganese porphyrin potentiates dexamethasone-induced apoptosis in lymphoma cells. Cancer Res. 2009; 69:5450–5457. [PubMed: 19549914]

116. Okado-Matsumoto A, Batinic-Haberle I, Fridovich I. Complementation of SOD-deficient Escherichia coli by manganese porphyrin mimics of superoxide dismutase activity. Free Radic Biol Med. 2004; 37:401–410. [PubMed: 15223074]

117. Tovmasyan AG, Rajic Z, Spasojevic I, Reboucas JS, Chen X, Salvemini D, Sheng H, Warner DS, Benov L, Batinic-Haberle I. Methoxy-derivatization of alkyl chains increases the in vivo efficacy of cationic Mn porphyrins Synthesis, characterization, SOD-like activity, and SOD-deficient E. coli study of meta Mn(III) N-methoxyalkylpyridylporphyrins. Dalton Trans. 2011; 40:4111–4121. [PubMed: 21384047]

118. Rajic Z, Tovmasyan A, Li AM, Gralla EB, Sheng H, Warner DS, Benov L, Spasojevic I, Batinic-Haberle I. A breakthrough in the development of SOD mimics/cellular redox modulators: a superior Mn porphyrin, MnTnBuOE-2-PyP^{5+} with finely tuned properties. Free Radic Biol Med. 2011; 51:S95.

119. Zhao Y, Chaiswing L, Velez JM, Batinic-Haberle I, Colburn NH, Oberley TD, St Clair DK. p53 translocation to mitochondria precedes its nuclear translocation and targets mitochondrial oxidative defense protein-manganese superoxide dismutase. Cancer Res. 2005; 65:3745–3750. [PubMed: 15867370]

120. Ferrer-Sueta G, Hannibal L, Batinic-Haberle I, Radi R. Reduction of manganese porphyrins by flavoenzymes and submitochondrial particles: a catalytic cycle for the reduction of peroxynitrite. Free Radic Biol Med. 2006; 41:503–512. [PubMed: 16843831]

121. Spasojevic I, Chen Y, Noel TJ, Yu Y, Cole MP, Zhang L, Zhao Y, St Clair DK, Batinic-Haberle I. Mn porphyrin-based superoxide dismutase (SOD) mimic, MnIIITE-2-PyP5+, targets mouse heart mitochondria. Free Radic Biol Med. 2007; 42:1193–1200. [PubMed: 17382200]

122. Spasojevic I, Miryala S, Tovmasyan A, Salvemini D, Vujaskovic Z, Batinic-Haberle I, St Clair D. Lipophilicity of Mn(III) N-alkylpyridylporphyrins dominates their accumulation within mitochondria and therefore in vivo efficacy. A mouse study. Free Radic Biol Med. 2011; 51:S98.

123. Beavis AD, Brannan RD, Garlid KD. Swelling and contraction of the mitochondrial matrix. I. A structural interpretation of the relationship between light scattering and matrix volume. J Biol Chem. 1985; 260:13424–13433. [PubMed: 4055741]

124. Cohen NS, Cheung CW, Raijman L. Measurements of mitochondrial volumes are affected by the amount of mitochondria used in the determinations. Biochem J. 1987; 245:375–379. [PubMed: 2444215]

125. Halestrap AP, Dunlop JL. Intramitochondrial regulation of fatty acid beta-oxidation occurs between flavoprotein and ubiquinone. A role for changes in the matrix volume. Biochem J. 1986; 239:559–565. [PubMed: 3827814]

126. Halestrap AP, Quinlan PT. The intramitochondrial volume measured using sucrose as an extramitochondrial marker overestimates the true matrix volume determined with mannitol. Biochem J. 1983; 214:387–393. [PubMed: 6412699]

127. Halestrap AP, Quinlan PT, Whipps DE, Armston AE. Regulation of the mitochondrial matrix volume in vivo and in vitro. The role of calcium. Biochem J. 1986; 236:779–787. [PubMed: 2431681]

128. Nedergaard J, Cannon B. Apparent unmasking of [3H]GDP binding in rat brown-fat mitochondria is due to mitochondrial swelling. Eur J Biochem. 1987; 164:681–686. [PubMed: 3569283]

129. Radi R, Turrens JF, Freeman BA. Cytochrome c-catalyzed membrane lipid peroxidation by hydrogen peroxide. Arch Biochem Biophys. 1991; 288:118–125. [PubMed: 1654818]

130. Rickwood, D.; Wilson, MT.; Darley-Usmar, VM. Mitochondria. IRL Press; Oxford: 1987.

131. Spasojevic I, Li AM, Tovmasyan A, Rajic Z, Salvemini D, St Clair D, Valentine JS, Vujaskovic Z, Gralla EB, Batinic-Haberle I. Accumulation of porphyrin-based SOD mimics in mitochondria is proportional to their lipophilicity. Free Radic Biol Med. 2010; 49:S199.

132. Spasojevic I, Kos I, Benov LT, Rajic Z, Fels D, Dedeugd C, Ye X, Vujaskovic Z, Reboucas JS, Leong KW, Dewhirst MW, Batinic-Haberle I. Bioavailability of metalloporphyrin-based SOD mimics is greatly influenced by a single charge residing on a Mn site. Free Radic Res. 2011; 45:188–200. [PubMed: 20942564]

133. Ferrer-Sueta G, Manta B, Botti H, Radi R, Trujillo M, Denicola A. Factors affecting protein thiol reactivity and specificity in peroxide reduction. Chem Res Toxicol. 2011; 24:434–450. [PubMed: 21391663]

134. Mouraviev V, Venkatraman TN, Tovmasyan A, Kimura M, Tsivian M, Mouravieva V, Polascik TJ, Wang H, Amrhein TJ, Batinic-Haberle I, Lascola C. Manganese porphyrins as novel molecular MRI contrast agents. J Endourol. 2011

135. Ferrer-Sueta G, Quijano C, Alvarez B, Radi R. Reactions of manganese porphyrins and manganese-superoxide dismutase with peroxynitrite. Methods Enzymol. 2002; 349:23–37. [PubMed: 11912912]

136. Ferrer-Sueta G, Vitturi D, Batinic-Haberle I, Fridovich I, Goldstein S, Czapski G, Radi R. Reactions of manganese porphyrins with peroxynitrite and carbonate radical anion. J Biol Chem. 2003; 278:27432–27438. [PubMed: 12700236]

137. Spasojevic I, Batinic-Haberle I, Fridovich I. Nitrosylation of manganese(II) tetrakis(N-ethylpyridinium-2-yl)porphyrin: a simple and sensitive spectrophotometric assay for nitric oxide. Nitric oxide. 2000; 4:526–533. [PubMed: 11020341]

138. Batinic-Haberle I, Spasojevic I, Fridovich I. Tetrahydrobiopterin rapidly reduces the SOD mimic Mn(III) ortho-tetrakis(N-ethylpyridinium-2-yl)porphyrin. Free Radic Biol Med. 2004; 37:367–374. [PubMed: 15223070]

139. Ferrer-Sueta G, Batinic-Haberle I, Spasojevic I, Fridovich I, Radi R. Catalytic scavenging of peroxynitrite by isomeric Mn(III) N-methylpyridylporphyrins in the presence of reductants. Chem Res Toxicol. 1999; 12:442–449. [PubMed: 10328755]

140. Coulter ED, Emerson JP, KurtzJr DM, Cabelli DE. Superoxide Reactivity of Rubredoxin Oxidoreductase (Desulfoferrodoxin) from Desulfovibrio vulgaris: A Pulse Radiolysis Study. J Am Chem Soc. 2000; 122:11555–11556.

141. Tian J, Peehl DM, Knox SJ. Metalloporphyrin synergizes with ascorbic acid to inhibit cancer cell growth through fenton chemistry. Cancer Biotherapy Radiopharm. 2010; 25:439–448.
142. Ye X, Fels D, Tovmasyan A, Aird KM, de Deugd C, Allensworth JL, Kos I, Park W, Spasojevic I, Devi GR, Dewhirst MW, Leong KW, Batinic-Haberle I. Cytotoxic effects of Mn(III) N-alkylpyridylporphyrins in the presence of cellular reductant, scorbate. Free Radic Res. 2011
143. Rabbani ZN, Spasojevic I, Zhang X, Moeller BJ, Haberle S, Vasquez-Vivar J, Dewhirst MW, Vujaskovic Z, Batinic-Haberle I. Antiangiogenic action of redox-modulating Mn(III) meso-tetrakis(N-ethylpyridinium-2-yl)porphyrin, MnTE-2-PyP(5+), via suppression of oxidative stress in a mouse model of breast tumor. Free Radic Biol Med. 2009; 47:992–1004. [PubMed: 19591920]
144. Dorai T, Fishman A, Ding C, Batinic-Haberle I, Goldfarb D, Grasso M. Amelioration of renal ischemia-reperfusion injury with a novel protective cocktail. J Urol. 2011
145. Goodman M, Bostick RM, Kucuk O, Jones DP. Clinical trials of antioxidants as cancer prevention agents: Past, present, and future. Free Radic Biol Med. 2011; 51:1068–1084. [PubMed: 21683786]
146. Kim A, Joseph S, Khan A, Epstein CJ, Sobel R, Huang TT. Enhanced expression of mitochondrial superoxide dismutase leads to prolonged in vivo cell cycle progression and up-regulation of mitochondrial thioredoxin. Free Radic Biol Med. 2010; 48:1501–1512. [PubMed: 20188820]
147. Khan I, Batinic-Haberle I, Benov LT. Effect of potent redox-modulating manganese porphyrin, MnTM-2-PyP, on the Na(+)/H(+) exchangers NHE-1 and NHE-3 in the diabetic rat. Redox Rep. 2009; 14:236–242. [PubMed: 20003708]
148. Moeller BJ, Batinic-Haberle I, Spasojevic I, Rabbani ZN, Anscher MS, Vujaskovic Z, Dewhirst MW. A manganese porphyrin superoxide dismutase mimetic enhances tumor radioresponsiveness. Int J Radiat Oncol Biol Phys. 2005; 63:545–552. [PubMed: 16168847]
149. Moeller BJ, Cao Y, Li CY, Dewhirst MW. Radiation activates HIF-1 to regulate vascular radiosensitivity in tumors: role of reoxygenation, free radicals, and stress granules. Cancer Cell. 2004; 5:429–441. [PubMed: 15144951]
150. Sheng H, Yang W, Fukuda S, Tse HM, Paschen W, Johnson K, Batinic-Haberle I, Crapo JD, Pearlstein RD, Piganelli J, Warner DS. Long-term neuroprotection from a potent redox-modulating metalloporphyrin in the rat. Free Radic Biol Med. 2009; 47:917–923. [PubMed: 19631268]
151. Tse HM, Milton MJ, Piganelli JD. Mechanistic analysis of the immunomodulatory effects of a catalytic antioxidant on antigen-presenting cells: implication for their use in targeting oxidation-reduction reactions in innate immunity. Free Radic Biol Med. 2004; 36:233–247. [PubMed: 14744635]
152. Piganelli JD, Flores SC, Cruz C, Koepp J, Batinic-Haberle I, Crapo J, Day B, Kachadourian R, Young R, Bradley B, Haskins K. A metalloporphyrin-based superoxide dismutase mimic inhibits adoptive transfer of autoimmune diabetes by a diabetogenic T-cell clone. Diabetes. 2002; 51:347–355. [PubMed: 11812741]
153. Bielski BHJ, Allen AO, Schwarz HA. Mechanism of the disproportionation of ascorbate radicals. J Am Chem Soc. 1981; 103:3516–3518.
154. Cabelli DE, Bielski BHJ. Kinetics and mechanism for the oxidation of ascorbic acid/ascorbate by HO2/O2- (hydroperoxyl/superoxide) radicals. A pulse radiolysis and stopped-flow photolysis study. J Phys Chem. 1983; 87:1809–1812.
155. Kobayashi N, Saiki H, Osa T. Catalytic electroreduction of molecular oxygen using [5,10,15,20-tetrakis-(1-methylpyridinium-4-yl)porphinato]manganese. Chem Lett. 1985; 14:1917–1920.
156. Miller DM, Buettner GR, Aust SD. Transition metals as catalysts of “autoxidation” reactions. Free Radic Biol Med. 1990; 8:95–108. [PubMed: 2182396]
157. Nadezhdin AD, Dunford HB. The oxidation of ascorbic acid and hydroquinone by perhydroxyl radicals. A flash photolysis study. Can J Chem. 1979; 57:3017–3022.
158. Nishikimi M. Oxidation of ascorbic acid with superoxide anion generated by the xanthine-xanthine oxidase system. Biochem Biophys Res Commun. 1975; 63:463–468. [PubMed: 235924]

159. Williams NH, Yandell JK. Outer-sphere electron-transfer reactions of ascorbate anions. Aust J Chem. 1982; 35:1133–1144.
160. Batinic-Haberle I, Benov LT. An SOD mimic protects NADP+-dependent isocitrate dehydrogenase against oxidative inactivation. Free Radic Res. 2008; 42:618–624. [PubMed: 18608518]
161. Kos I, Ali DK, Oriowo M, Batinic-Haberle I, Benov L. Timely administration of Mn porphyrin, MnTM-2-PyP^{5+} is critical to afford protection in diabetes. A rat study. Free Radic Biol Med. 2011; 51:S90.
162. Sheng H, Spasojevic I, Warner DS, Batinic-Haberle I. Mouse spinal cord compression injury is ameliorated by intrathecal cationic manganese(III) porphyrin catalytic antioxidant therapy. Neurosci Lett. 2004; 366:220–225. [PubMed: 15276251]
163. Drobyshevsky A, Luo K, Derrick M, Yu L, Prasad PV, Vasquez-Vivar J, Batinic-Haberle I, Tan S. Oxidants in fetal brain reperfusion-reoxygenation injury trigger motor deficits. Ann Neurol. 2011
164. Ahmad IM, Aykin-Burns N, Sim JE, Walsh SA, Higashikubo R, Buettner GR, Venkataraman S, Mackey MA, Flanagan SW, Oberley LW, Spitz DR. Mitochondrial O2*- and H2O2 mediate glucose deprivation-induced stress in human cancer cells. J Biol Chem. 2005; 280:4254–4263. [PubMed: 15561720]
165. Aykin-Burns N, Ahmad IM, Zhu Y, Oberley LW, Spitz DR. Increased levels of superoxide and H2O2 mediate the differential susceptibility of cancer cells versus normal cells to glucose deprivation. Biochem J. 2009; 418:29–37. [PubMed: 18937644]
166. Bras A, Sanches R, Cristovao L, Fidalgo P, Chagas C, Mexia J, Leitao N, Rueff J. Oxidative stress in familial adenomatous polyposis. Eur J Cancer Prev. 1999; 8:305–310. [PubMed: 10493305]
167. Devi GS, Prasad MH, Saraswathi I, Raghu D, Rao DN, Reddy PP. Free radicals antioxidant enzymes and lipid peroxidation in different types of leukemias. Clin Chim Acta. 2000; 293:53–62. [PubMed: 10699422]
168. Hileman EO, Liu J, Albitar M, Keating MJ, Huang P. Intrinsic oxidative stress in cancer cells: a biochemical basis for therapeutic selectivity. Cancer Chemother Pharmacol. 2004; 53:209–219. [PubMed: 14610616]
169. Ishii T, Yasuda K, Akatsuka A, Hino O, Hartman PS, Ishii N. A mutation in the SDHC gene of complex II increases oxidative stress, resulting in apoptosis and tumorigenesis. Cancer Res. 2005; 65:203–209. [PubMed: 15665296]
170. Kawanishi S, Hiraku Y, Pinlaor S, Ma N. Oxidative and nitrative DNA damage in animals and patients with inflammatory diseases in relation to inflammation-related carcinogenesis. Biol Chem. 2006; 387:365–372. [PubMed: 16606333]
171. Kondo S, Toyokuni S, Iwasa Y, Tanaka T, Onodera H, Hiai H, Imamura M. Persistent oxidative stress in human colorectal carcinoma, but not in adenoma. Free Radic Biol Med. 1999; 27:401–410. [PubMed: 10468215]
172. Pelicano H, Carney D, Huang P. ROS stress in cancer cells and therapeutic implications. Drug Resist Updat. 2004; 7:97–110. [PubMed: 15158766]
173. Szatrowski TP, Nathan CF. Production of large amounts of hydrogen peroxide by human tumor cells. Cancer Res. 1991; 51:794–798. [PubMed: 1846317]
174. Toyokuni S. Oxidative stress and cancer: the role of redox regulation. Biotherapy. 1998; 11:147–154. [PubMed: 9677046]
175. Toyokuni S, Okamoto K, Yodoi J, Hiai H. Persistent oxidative stress in cancer. FEBS Lett. 1995; 358:1–3. [PubMed: 7821417]
176. Wu LL, Chiou CC, Chang PY, Wu JT. Urinary 8-OHdG: a marker of oxidative stress to DNA, a risk factor for cancer, therosclerosis and diabetics. Clin Chim Acta. 2004; 339:1–9. [PubMed: 14687888]
177. Zhou Y, Hileman EO, Plunkett W, Keating MJ, Huang P. Free radical stress in chronic lymphocytic leukemia cells and its role in cellular sensitivity to ROS-generating anticancer agents. Blood. 2003; 101:4098–4104. [PubMed: 12531810]

178. Zhao Y, Chaiswing L, Oberley TD, Batinic-Haberle I, St Clair W, Epstein CJ, St Clair D. A mechanism-based antioxidant approach for the reduction of skin carcinogenesis. Cancer Res. 2005; 65:1401–1405. [PubMed: 15735027]

179. Petros JA, Baumann AK, Ruiz-Pesini E, Amin MB, Sun CQ, Hall J, Lim S, Issa MM, Flanders WD, Hosseini SH, Marshall FF, Wallace DC. mtDNA mutations increase tumorigenicity in prostate cancer. Proc Natl Acad Sci USA. 2005; 102:719–724. [PubMed: 15647368]

180. Kumar B, Koul S, Khandrika L, Meacham RB, Koul HK. Oxidative stress is inherent in prostate cancer cells and is required for aggressive phenotype. Cancer Res. 2008; 68:1777–1785. [PubMed: 18339858]

181. Baker AM, Oberley LW, Cohen MB. Expression of antioxidant enzymes in human prostatic adenocarcinoma. Prostate. 1997; 32:229–233. [PubMed: 9288180]

182. Bostwick DG, Alexander EE, Singh R, Shan A, Qian J, Santella RM, Oberley LW, Yan T, Zhong W, Jiang X, Oberley TD. Antioxidant enzyme expression and reactive oxygen species damage in prostatic intraepithelial neoplasia and cancer. Cancer. 2000; 89:123–134. [PubMed: 10897009]

183. Sun Y, St Clair DK, Xu Y, Crooks PA, St Clair WH. A NADPH oxidase-dependent redox signaling pathway mediates the selective radiosensitization effect of parthenolide in prostate cancer cells. Cancer Res. 2010; 70:2880–2890. [PubMed: 20233868]

184. Liao D, Johnson RS. Hypoxia: a key regulator of angiogenesis in cancer. Cancer Metastasis Rev. 2007; 26:281–290. [PubMed: 17603752]

185. Lu X, Kang Y. Hypoxia and hypoxia-inducible factors: master regulators of metastasis. Clin Cancer Res. 2010; 16:5928–5935. [PubMed: 20962028]

186. Beck R, Pedrosa RC, Dejeans N, Glorieux C, Leveque P, Gallez B, Taper H, Eeckhoudt S, Knoops L, Calderon PB, Verrax J. Ascorbate/menadione-induced oxidative stress kills cancer cells that express normal or mutated forms of the oncogenic protein Bcr-Abl. An in vitro and in vivo mechanistic study. Invest New Drugs. 2011; 29:891–900. [PubMed: 20454833]

187. Beck R, Verrax J, Gonze T, Zappone M, Pedrosa RC, Taper H, Feron O, Calderon PB. Hsp90 cleavage by an oxidative stress leads to its client proteins degradation and cancer cell death. Biochem Pharmacol. 2009; 77:375–383. [PubMed: 19014912]

188. Reuter S, Gupta SC, Chaturvedi MM, Aggarwal BB. Oxidative stress, inflammation, and cancer: how are they linked? Free Radic Biol Med. 2010; 49:1603–1616. [PubMed: 20840865]

189. Verrax J, Beck R, Dejeans N, Glorieux C, Sid B, Pedrosa RC, Benites J, Vasquez D, Valderrama JA, Calderon PB. Redox-active quinones and ascorbate: an innovative cancer therapy that exploits the vulnerability of cancer cells to oxidative stress. Anti-cancer Agents Med Chem. 2011; 11:213–221.

190. Wise-Faberowski L, Warner DS, Spasojevic I, Batinic-Haberle I. Effect of lipophilicity of Mn (III) ortho N-alkylpyridyl-diortho N, N′-diethylimidazolylporphyrins in two in-vitro models of oxygen and glucose deprivation-induced neuronal death. Free Radic Res. 2009; 43:329–339. [PubMed: 19259881]

191. Yu, L.; Ji, X.; Derrick, M.; Drobyshevsky, A.; Liu, T.; Batinic-Haberle, I.; Tan, S. Testing new porphyrins in in vivo model Ssystems: effect of Mn porphyrins in animal model of cerebral palsy. 6th International Conference on Porphyrins and Phthalocyanines; New Mexico. 2010.

192. Keir ST, Dewhirst MW, Kirkpatrick JP, Bigner DD, Batinic-Haberle I. Cellular redox modulator, ortho Mn(III) meso-tetrakis(N-n-hexylpyridinium-2-yl)porphyrin, MnTnHex-2-PyP(5+) in the treatment of brain tumors. Anti-cancer Agents Med Chem. 2011; 11:202–212.

193. Dogan S, Unal M, Ozturk N, Yargicoglu P, Cort A, Spasojevic I, Batinic-Haberle I, Aslan M. Manganese porphyrin reduces retinal injury induced by ocular hypertension in rats. Exp Eye Res. 2011

194. Gauter-Fleckenstein B, Fleckenstein K, Owzar K, Jiang C, Batinic-Haberle I, Vujaskovic Z. Comparison of two Mn porphyrin-based mimics of superoxide dismutase in pulmonary radioprotection. Free Radic Biol Med. 2008; 44:982–989. [PubMed: 18082148]

195. Saba H, Batinic-Haberle I, Munusamy S, Mitchell T, Lichti C, Megyesi J, MacMillan-Crow LA. Manganese porphyrin reduces renal injury and mitochondrial damage during ischemia/reperfusion. Free Radic Biol Med. 2007; 42:1571–1578. [PubMed: 17448904]

196. Pollard JM, Reboucas JS, Durazo A, Kos I, Fike F, Panni M, Gralla EB, Valentine JS, Batinic-Haberle I, Gatti RA. Radioprotective effects of manganese-containing superoxide dismutase mimics on ataxia-telangiectasia cells. Free Radic Biol Med. 2009; 47:250–260. [PubMed: 19389472]

197. Benov L, Craik J, Batinic-Haberle I. Protein damage by photo-activated Zn(II) N-alkylpyridylporphyrins. Amino acids. 2010

198. Bakthavatchalu V, Dey S, Xu Y, Noel T, Jungsuwadee P, Holley AK, Dhar SK, Batinic-Haberle I, St Clair DK. Manganese superoxide dismutase is a mitochondrial fidelity protein that protects Polgamma against UV-induced inactivation. Oncogene. 2011

199. Graziewicz MA, Longley MJ, Bienstock RJ, Zeviani M, Copeland WC. Structure-function defects of human mitochondrial DNA polymerase in autosomal dominant progressive external ophthalmoplegia. Nat Struct Mol Biol. 2004; 11:770–776. [PubMed: 15258572]

200. Wu S, Wang L, Jacoby AM, Jasinski K, Kubant R, Malinski T. Ultraviolet B light-induced nitric oxide/peroxynitrite imbalance in keratinocytes--implications for apoptosis and necrosis. Photochem Photobiol. 2010; 86:389–396. [PubMed: 20074088]

201. Doyle T, Bryant L, Batinic-Haberle I, Little J, Cuzzocrea S, Masini E, Spasojevic I, Salvemini D. Supraspinal inactivation of mitochondrial superoxide dismutase is a source of peroxynitrite in the development of morphine antinociceptive tolerance. Neuroscience. 2009; 164:702–710. [PubMed: 19607887]

202. Muscoli C, Cuzzocrea S, Ndengele MM, Mollace V, Porreca F, Fabrizi F, Esposito E, Masini E, Matuschak GM, Salvemini D. Therapeutic manipulation of peroxynitrite attenuates the development of opiate-induced antinociceptive tolerance in mice. J Clin Invest. 2007; 117:3530–3539. [PubMed: 17975673]

203. Aycicek A, Iscan A. Oxidative and antioxidative capacity in children with cerebral palsy. Brain Res Bull. 2006; 69:666–668. [PubMed: 16716836]

204. Baud O, Haynes RF, Wang H, Folkerth RD, Li J, Volpe JJ, Rosenberg PA. Developmental up-regulation of MnSOD in rat oligodendrocytes confers protection against oxidative injury. Eur J Neurosci. 2004; 20:29–40. [PubMed: 15245476]

Highlights

- MnSOD action was briefly summarized and compared to the action of its mimics
- Mn porphyrins and MitoQ were described in details
- Cationic Mn(III) *N*-alkylpyridylporphyrins mimic both the catalytic action and location of MnSOD
- MitoQ accumulates in mitochondria and scavenges superoxide stoichiometrically

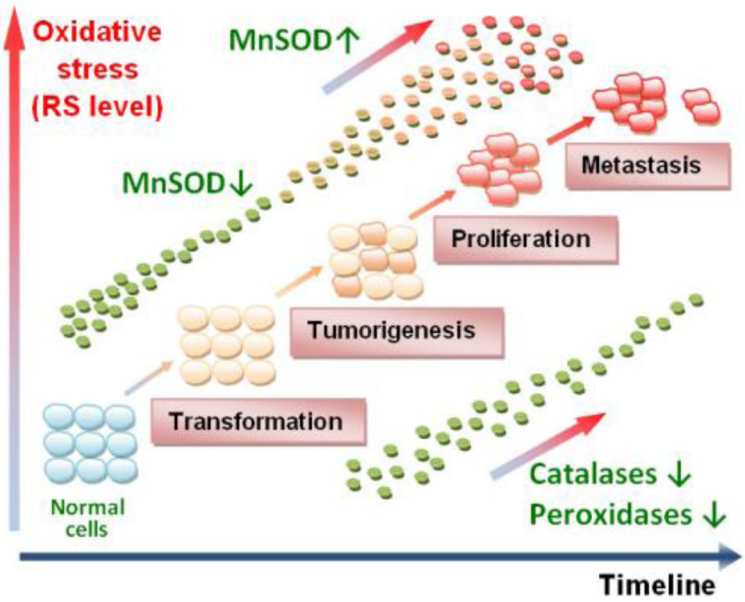

Figure 1.

A simplified presentation of the role of MnSOD under physiological and pathological conditions. The possible scenario presented here aims at reconciliation of the dichotomous role of MnSOD as tumor suppressor (antioxidant) or oncogene (pro-oxidant). The differences in these two opposing roles are likely related to the different redox-status of the cell, primarily the ratio of the endogenous antioxidants that controls $O_2^{\cdot-}/H_2O_2$ ratio. The common understanding is that cells which have intrinsically lower levels of MnSOD are under oxidative stress and may eventually transform into cancer cells. Further, when exposure to either single or multiple oxidative insults transforms cells prior to their becoming malignant, MnSOD levels are low and the cells are consequently under oxidative stress. The impaired redox status would in turn result in higher oxidative damage of biological targets, nucleic acids included, which would amplify mutations and enforce tumorigenesis. Once the process starts, the oxidative stress is perpetuated and the cell fights it by upregulation of MnSOD. The reportedly reduced ability of a malignant cell to remove H_2O_2 [32–36] further perpetuates the oxidative stress, and MnSOD would appear as an oncogene. Tumor utilizes increased levels of peroxide to signal the activation of transcription factors and upregulation of those proteins (such as HIF-1α, VEGF, NADPH oxidases), which would maintain its oxidative stress and facilitate its progression and metastasis [1]. The complex role of MnSOD in maintaing the cellular redox status, via both its traditional role and by modulating cellular production of H_2O_2, has been elaborated by Buetner et al [16], while St Clair group has recently [38] pointed to the critical role of Sp1 and p53 in early and late stages of tumorigenesis on levels of MnSOD expression. **- normal cell; - transformed cell; - cancer cell.**

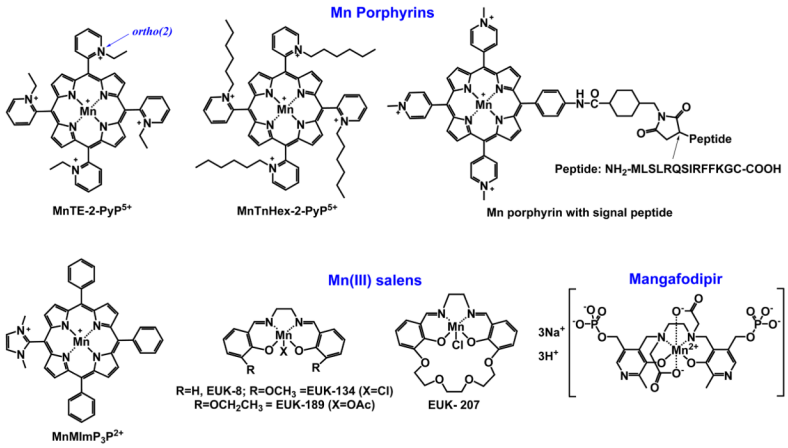

Figure 2.
Chemical structures of mitochondrially-targeted metal based SOD mimics.

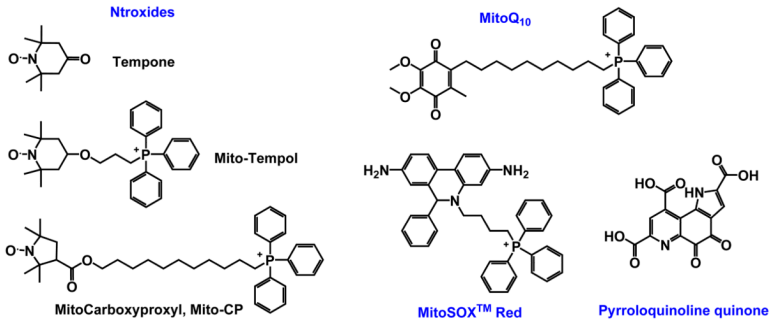

Figure 3.
Structures of mitochondrially-targeted non-metal based SOD mimics.

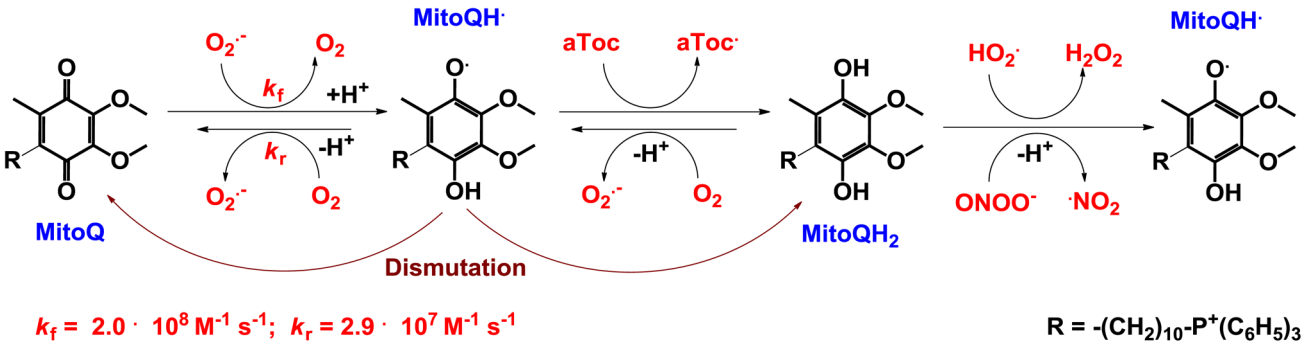

Figure 4.

The mechanism of action of MitoQ with respect to scavenging $O_2^{\cdot-}$. These redox reactions are similar to those of ubiquinone in mitochondrial electron transport chain, and are responsible for the production of low levels of superoxide.

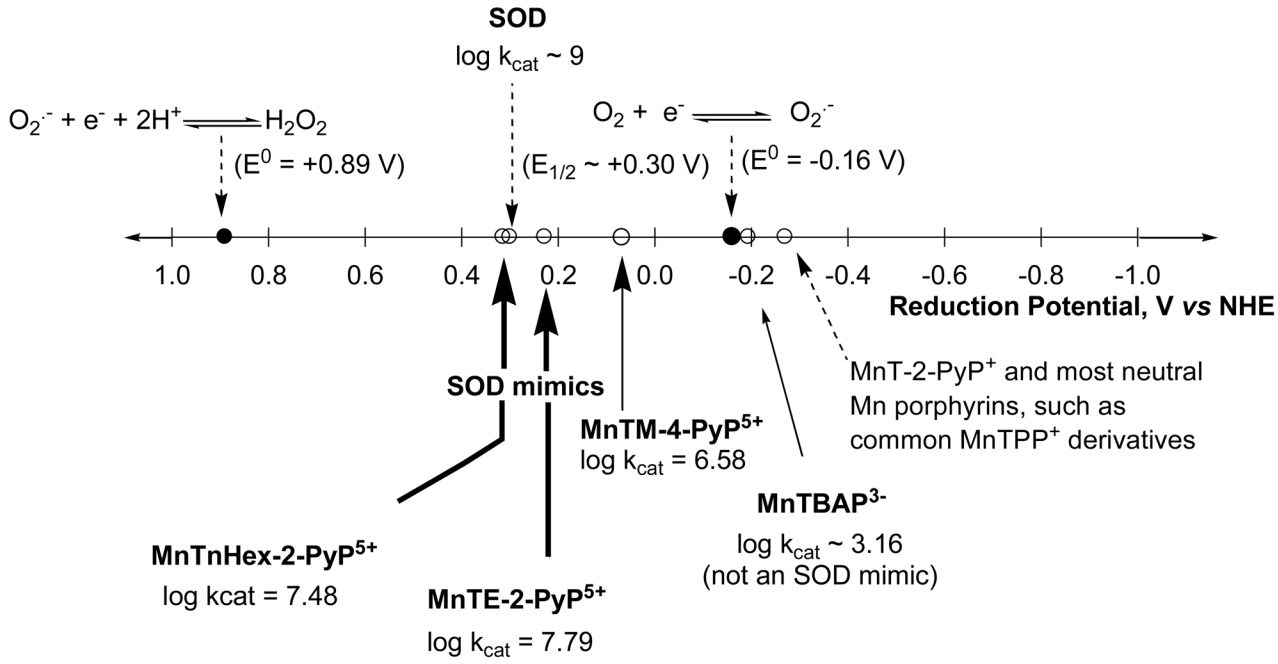

Figure 5.

The design of SOD mimics was based on the same thermodynamics and electrostatics which play critical roles in enzyme catalysis. Potent SOD mimics are those that have $E_{1/2}$ for M^{III}/M^{II} redox couple in the vicinity of the $E_{1/2}$ of SOD enzymes, ~ +300 mV *vs* NHE. All SOD enzymes regardless of the metal site, whether Mn, Fe, Cu or Ni, redox cycle at same potentials [107, 111]. Modified from ref [45].

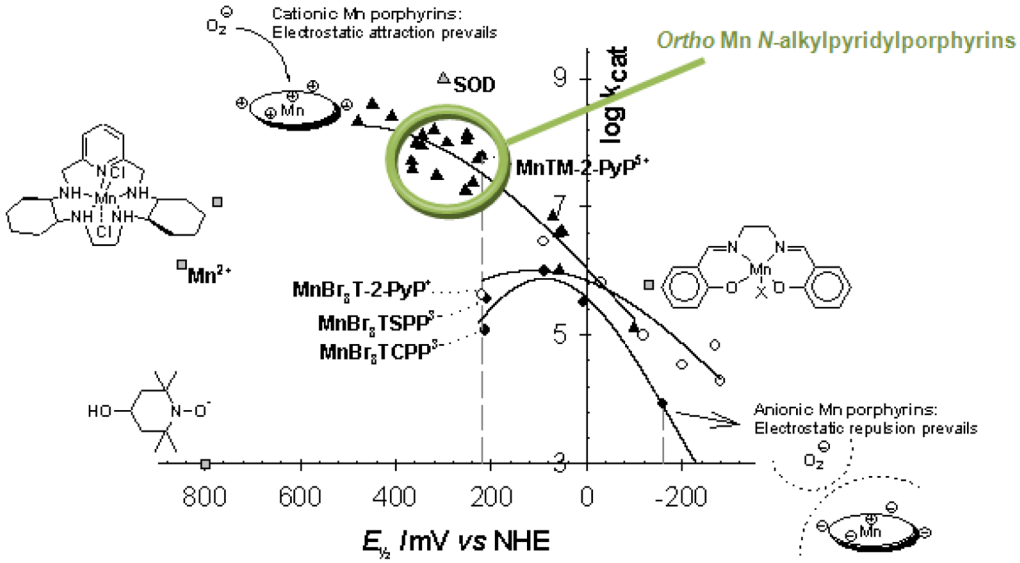

Figure 6.

Structure-activity relationship between the metal centered reduction potential, $E_{1/2}$ for $Mn^{III}/Mn^{II}P$ redox couple for cationic, neutral and anionic Mn porphyrins, and $k_{cat}(O_2^{\cdot-})$. At around +200 mV *vs* NHE, the k_{cat} is ≥2 higher for cationic than for neutral and anionic Mn porphyrins, indicating a vast contribution by electrostatics in the catalysis of $O_2^{\cdot-}$ dismutation. Modified from ref [82].

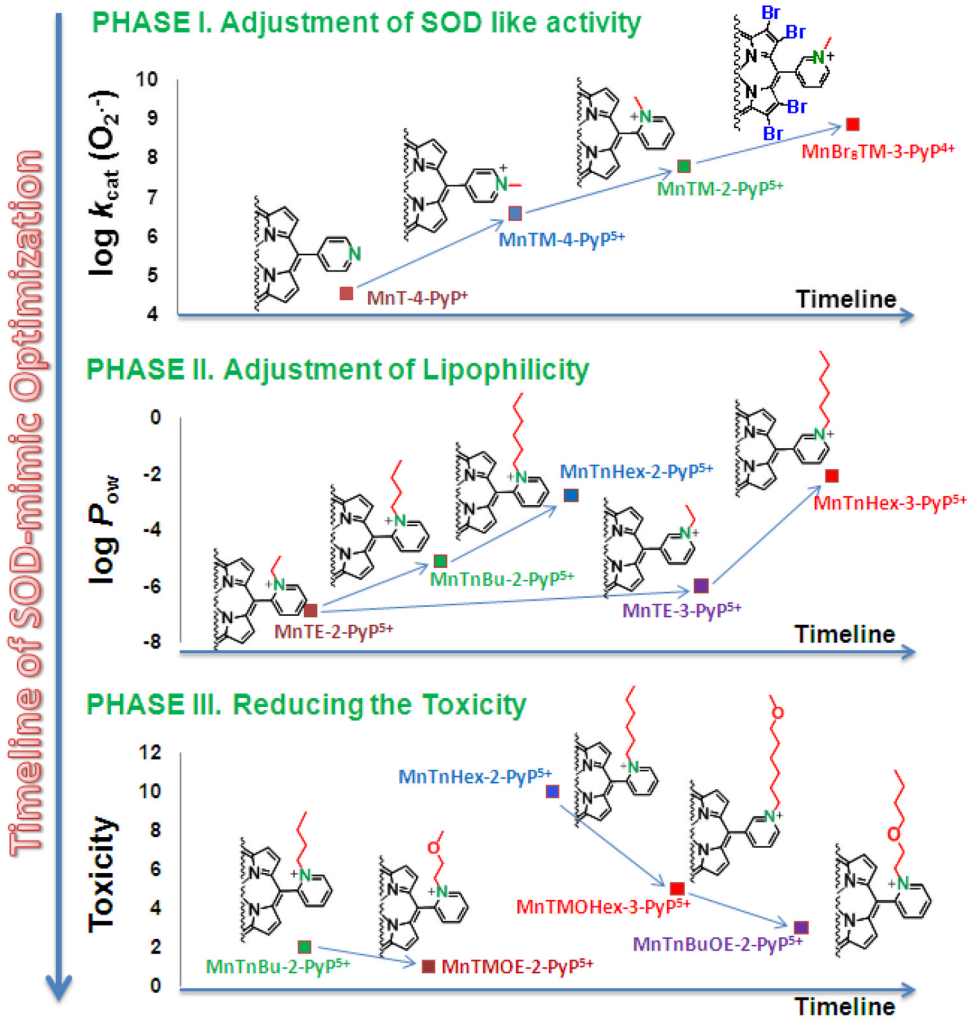

Figure 7.

The timeline for the optimization of the Mn porphyrin-based cellular redox modulators. **Phase I** studies were directed primarily toward generating compounds with high $k_{cat}(O_2^{\cdot-})$, and were successfully accomplished. Pentacationic MnTE-2-PyP^{5+} has been identified as our lead compound. As the research progressed, the clinical relevance of such an excessively charged drug was questioned. To address this issue, analytical tools were developed to assess the pharmacokinetics of MnPs and their subcellular distribution. The first data indicate that even the fairly hydrophilic MnTE-2-PyP^{5+} targets mitochondria and crosses the BBB. In **Phase II** the MnP structure was modified to enhance its bioavailability, primarily lipophilicity, in order to increase its transport across the BBB and mitochondrial accumulation. Lipophilicity was enhanced 10-fold: (1) by moving ethyl groups from *ortho* to *meta* positions; and (2) by lengthening the alkyl chains by each additional carbon atom. Presently, **Phase III** efforts are directed toward reducing toxicity of MnPs, while maintaining high redox activity and lipophilicity. Longer-alkyl chain analogues possess surfactant-based toxicity. Such toxicity was suppressed by disrupting the hydrophobicity of alkyl chains via introduction of oxygen atoms: (1) at the alkyl chain periphery, and (2) closer to the pyridyl nitrogens. In the first case, with MnTMOHex-2-PyP^{5+} an unfavorable drop in hydrophobicity was observed relative to MnTnHex-2-PyP^{5+} [109, 117], while in the second case, with MnTnBuOE-2-PyP^{5+}, not only was a high lipopohilicity preserved, but

also a slight gain in catalytic potency was achieved when compared to MnTnHex-2-PyP^{5+} [118].

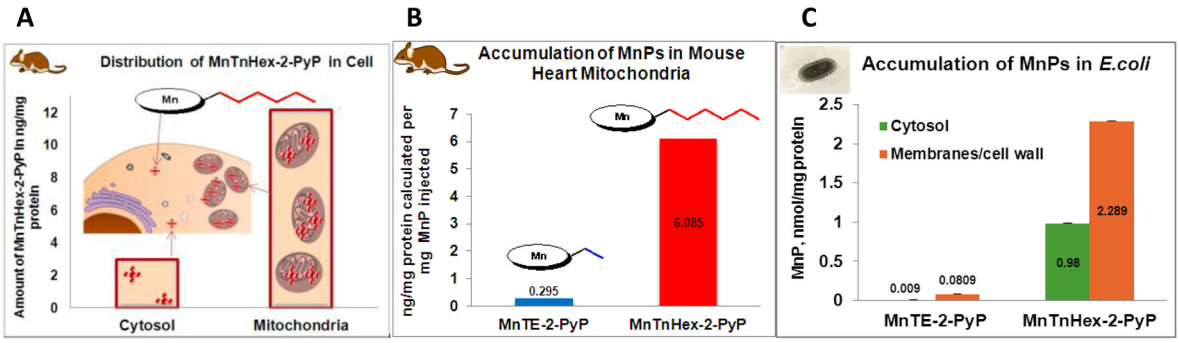

Figure 8.

(A) Accumulation of MnTnHex-2-PyP^{5+} in C57BL/6 mouse heart cytosol and mitochondria at 6 hours after single ip injection of 2 mg/kg. Data obtained using the LC/ESI-MS/MS method [121]. **(B)** Comparison of the accumulation of hydrophilic MnTE-2-PyP^{5+} and lipophilic MnTnHex-2-PyP^{5+} in C57BL/6 mouse heart mitochondria at 6 hours after single ip injection. **(C)** The accumulation of MnTE-2-PyP^{5+} and MnTnHex-2-PyP^{5+} in wild type AB1157 *E. coli* membranes/cell wall (envelope) and cytosol after *E. coli* was incubated for 1 hour in the presence of 5 μM Mn porphyrins in M9CA medium [91]. One of the present evolutionary hypotheses is that eukaryotic mitochondrial membranes and matrix are derived from *E. coli* envelope and cytosol, respectively [83]. Thus, the biodistribution within *E. coli* resembles the biodistribution within heart mitochondria.

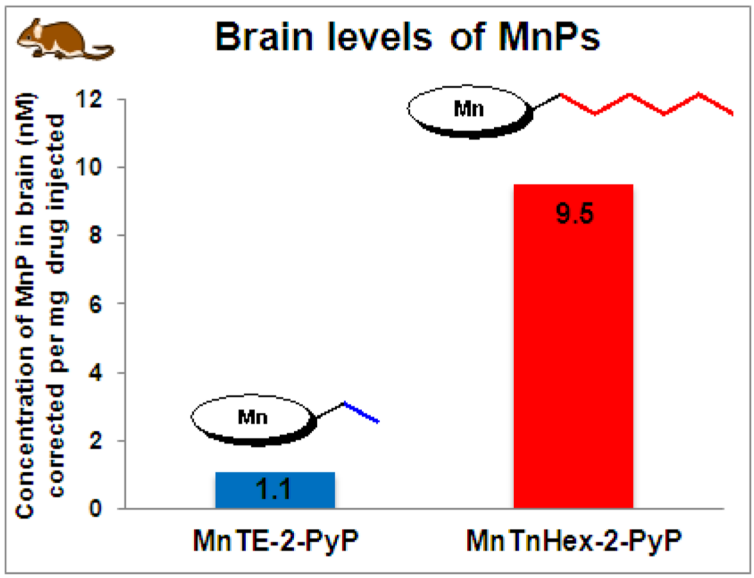

Figure 9.

The distribution of MnTE-2-PyP^{5+} and MnTnHex-2-PyP^{5+} in murine brain at 24 hours after single ip injection [112]. Brain levels of lipophilic MnTnHex-2-PyP^{5+} are 9-fold higher than of hydrophilic MnTE-2-PyP^{5+}.

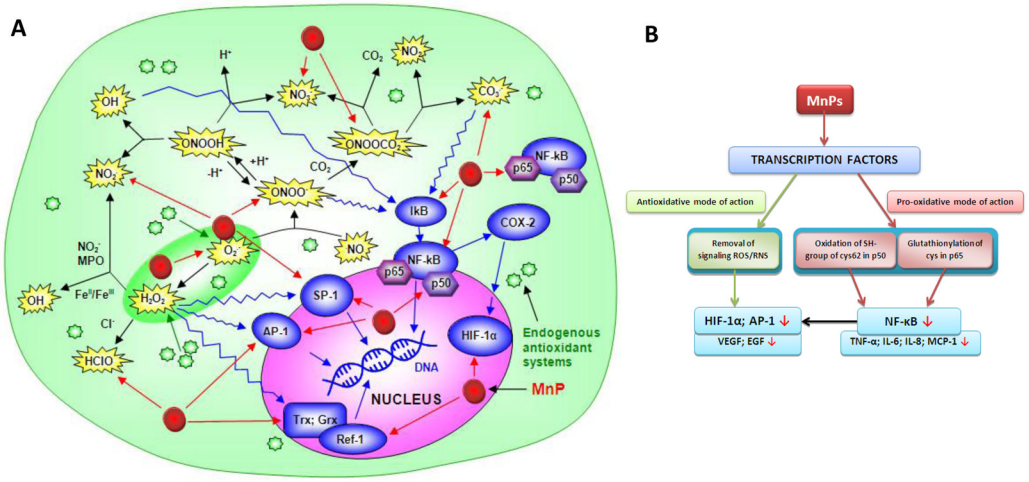

Figure 10.

The reactivity of Mn porphyrins toward reactive species (**A**) and transcription factors (**B**). The reactivity of Mn(III) substituted pyridyl(or imidazolyl)porphyrins toward several oxygen and nitrogen species, such as $O_2^{\cdot-}$, $ONOO^-$, ClO^-, $^{\cdot}NO_2$, $CO_3^{\cdot-}$, would produce antioxidative effects [44–46]. Under physiological conditions, H_2O_2 formed during dismutation is removed by abundant peroxide-removing systems. The $ONOO^-$ reacts with MnTE-2-PyP^{5+} which has Mn in +3 (k_{red} = 3.4 × 10^7 M^{-1} s^{-1} at 37°C), and with MnTE-2-PyP^{4+} that contains Mn in +2 oxidation states ($k \gg 10^7$ M^{-1} s^{-1} at 37°C) [135, 136]. MnTE-2-PyP^{5+} reacts also with $^{\cdot}NO$ ($k \sim 10^6$ M^{-1} s^{-1}) [137]. Based on the preliminary data, MnTE-2-PyP^{5+} reacts rapidly with ClO^- with a rate constant of $k \gg 10^6$ $M^{-1}s^{-1}$ [Ferrer-Sueta et al., unpublished]. Based on the thermodynamic and kinetic data thus far published on *ortho* isomers, those MnPs that are potent SOD mimics would likely favor reaction with $^{\bullet}NO_2$ too.

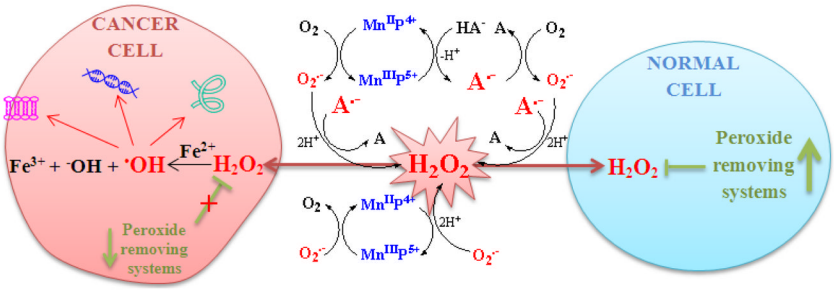

Figure 11.

The generation of the reactive oxygen species by Mn porphyrins coupled to ascorbate redox cycling. With abundant peroxide-removing systems, such action would generate antioxidative effects. Yet, if peroxide-removing enzymes are reduced, the H_2O_2 levels may increase and activate cellular transcription, which would in turn perpetuate oxidative stress. Under such conditions, the ability of MnPs to catalyze ascorbate oxidation would contribute to the progression of oxidative stress. The metal site of Mn porphyrin redox cycles between Mn +3 and +2 oxidation states while transferring electron to ascorbate and producing ascorbyl radical, $A^{\bullet -}$. The reoxidation of $Mn^{II}P$ to $Mn^{III}P$ may occur with O_2 or $O_2^{\bullet -}$, and in either case H_2O_2 would be eventually produced. The same is valid for the self-dismutation of $A^{\bullet -}$ and $O_2^{\bullet -}$, the reaction of $A^{\bullet -}$, HA^- and A^{2-} with $O_2^{\bullet -}$, and the reaction of $A^{\bullet -}$ with O_2 [153–159]. The type of outcome, antioxidant or pro-oxidative, would depend upon the cellular redox status, the levels of cellular endogenous defenses, SODs and peroxide-removing enzymes, levels of reactive species that MnP would encounter, levels of MnP and their site of accumulation. Modified from ref [142].

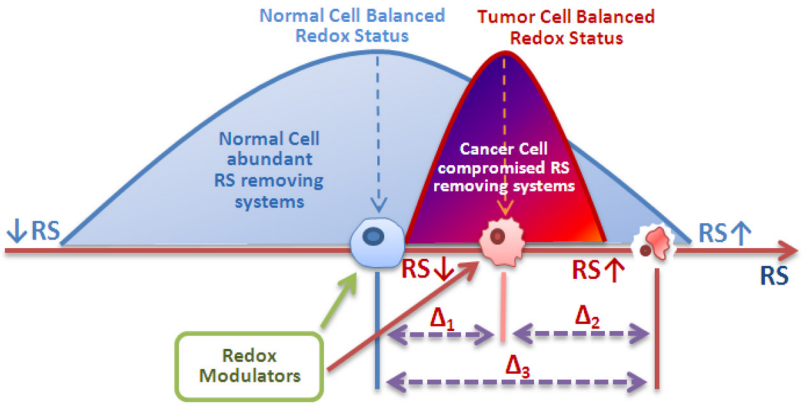

Figure 12.

Tumor growth/suppression by MnP is a function of oxidative stress/levels of reactive species (RS). Depending on the level of RS, different cellular events happen: at lower, physiological RS levels, signaling events predominate; while at very high levels oxidative events prevail. These scenarios are depicted by two bell shape curves for the normal and cancer cells. A tumor is frequently under oxidative stress, a “physiological” status that is visualized here by the maximum of its bell shape curve shifted towards higher RS levels. The increased level of RS is a signal for the upregulation of the genes needed to support tumor angiogenesis and progression [184, 185]. However, a tumor is vulnerable, and any further increase in oxidative burden would force tumor cells to undergo death. The strategy to treat tumors may be either to remove RS or to vastly increase their levels [27, 95]. The latter strategy has already been used in clinic; one example is the combination of ascorbate and the redox cycling agent menadione which results in increased peroxide levels. Parthenolide also has such a pro-oxidative effect, which is exerted by the selective upregulation of NADPH oxidases [186–190]. HIF-1α inhibition, and subsequent suppression of angiogenesis, is a part of the first strategy where MnP scavenges RS, and thereby affects cell signaling [143, 149].

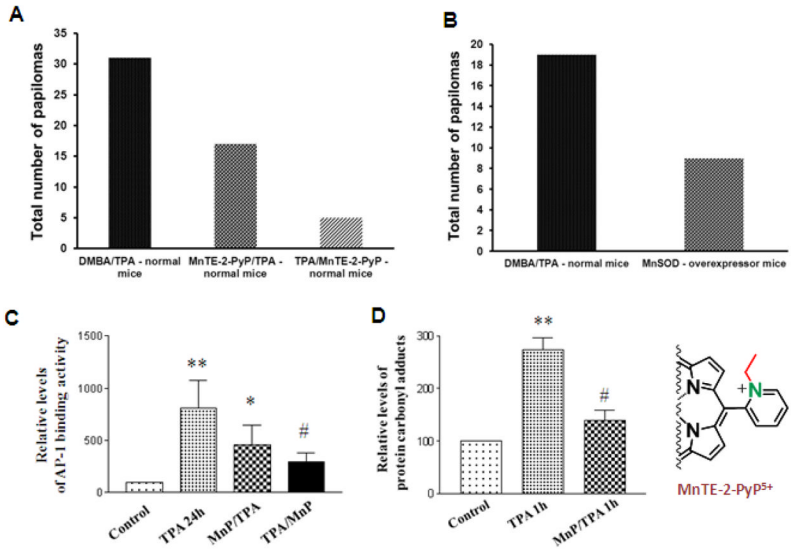

Figure 13.

MnTE-2-PyP^{5+} mimics MnSOD in suppressing skin carcinogenesis. The reduction in incidence and multiplicity of tumors (**A** and **B**) was achieved by inhibiting AP-1 activation (**C**), presumably *via* removing signaling species, which in turn suppresses oxidative stress as observed by reduction of protein carbonyl formation (**D**). Tumor was induced with 7,12-dimethylbenz (*a*)-anthracene (DMBA). TPA is a tumor promoter 12-*O*-tetradecanoylphorbol-13-acetate. MnTE-2-PyP^{5+} (MnP) was injected in two ways, before both apoptosis and proliferation (MnP/TPA), and after apoptosis and before proliferation (TPA/MnP). In the latter case, MnP did not attenuate apoptosis, but reduced proliferation, and therefore the effect was much more pronounced than in the former case (**A**). With MnSOD-overexpressor mice, MnSOD attenuated both apoptotic and proliferative pathways (**B**), which diminished the enzyme effect upon cancer incidence relative to the effect of timely administered MnSOD mimic. Modified from refs [20, 178].

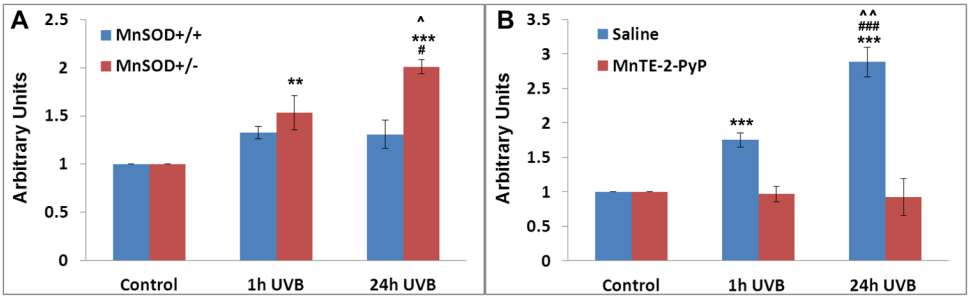

Figure 14.

The mouse model of UVB radiation-induced oxidative damage. MnSOD$^{+/+}$ wild type and heterozygous MnSOD knockout mice, MnSOD$^{+/-}$ were studied. The UVB radiation caused nitration and subsequent inactivation of polyγ, a polymerase enzyme responsible for the replication and repair of mtDNA. With MnSOD$^{+/+}$ mice, the oxidative damage was significantly reduce, and was fully suppressed when mice were treated with 5 mg/kg of MnTE-2-PyP^{5+} ip twice daily for 2 days before radiation. Quantification of polyγ co-immunoprecipitation by anti-3-nitrotyrosine antibody in mice skin lysates in terms of arbitrary units, is shown. **P < 0.01, ***P < 0.001 compared with control; $^{\#\#\#}$P < 0.001 compared between 1 hour and 24 hours after UVB treatment, $^{\#}$P < 0.05 compared between 1 hour and 24 hours after UVB treatment; ^P < 0.05 compared between MnSOD$^{+/+}$ and MnSOD$^{+/-}$ mice; ^^P < 0.01 compared between Mn^{III}TE-2-PyP^{5+} and saline pre-treatment. Modified from ref [198].

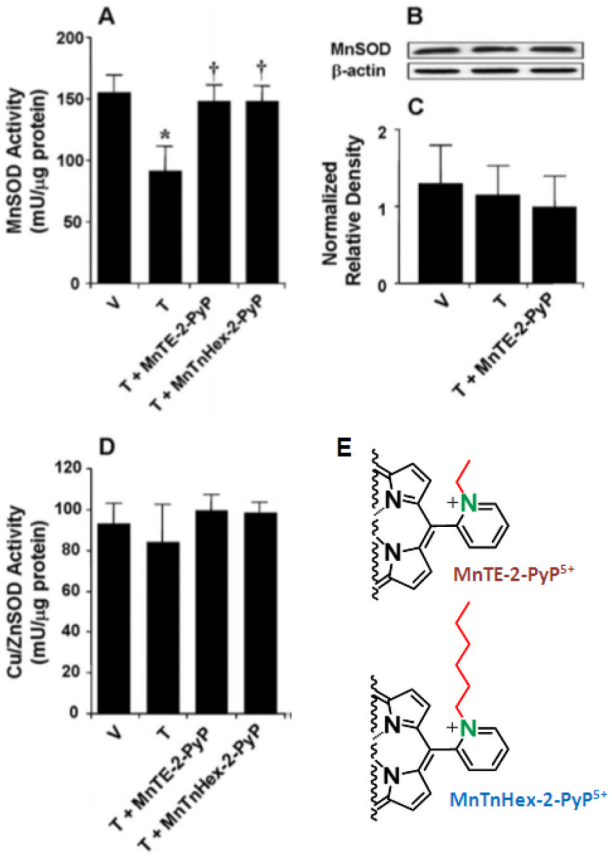

Figure 15.

The mouse model of chronic morphine tolerance. Mn porphyrins were able to either substitute for or protect MnSOD from inactivation in a mouse whole brain homogenate when injected ip at 3 mg/kg (MnTE-2-PyP^{5+}) and 0.1 mg/kg (MnTnHex-2-PyP^{5+}) for 4 days along with morphine. No effect was seen on the expression of MnSOD protein. T describes tolerant group (which develops chronic morphine tolerance), and V is a vehicle group. The 30-fold increased efficacy of MnTnHex-2-PyP^{5+} resembles its 20-fold increased mitochondrial accumulation relative to MnTE-2-PyP^{5+}. The higher ability of MnTnHex-2-PyP^{5+} to cross BBB further potentiates its effect in comparison with MnTE-2-PyP^{5+}. Modified from ref [201].

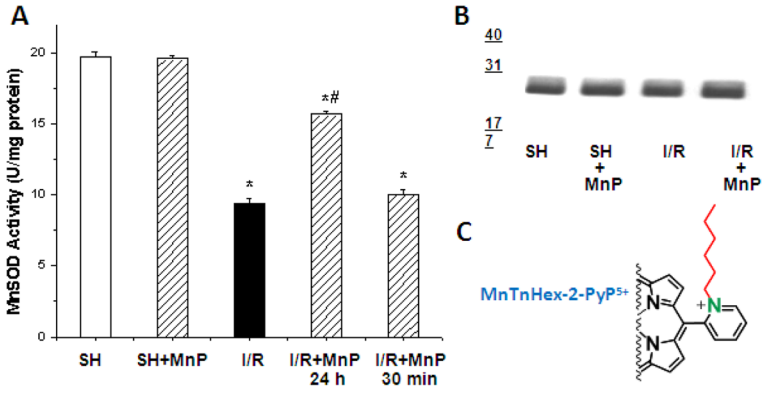

Figure 16.

The rat renal ischemia/reperfusion model. MnTnHex-2-PyP^{5+} (MnP) preserved MnSOD activity but did not affect protein expression. It was given iv into penil vein, at 0.05 mg/kg 30 minutes and 24 hours before ischemia/reperfusion. SH describes sham, and I/R ischemia/reperfusion. Modified from ref [195].

Table 1

The log k_{cat} for $O_2^{\cdot-}$ dismutation, $E_{1/2}$, metal-centered reduction potential for M^{III}/M^{II} redox couple (where M stands for metal) and the lipophilicity of SOD mimics expressed in terms of their partition between n-octanol and water, log P_{OW}. The P_{OW} values for $MitoQ_{10}$ and CoQ_{10} relate to distribution between n-octanol and PBS. Some other compounds that are mentioned in the text, but are not SOD mimics and/or no data exist on their mitochondrial accumulation, are listed also for comparison, and are indicated with "*".

Compound	$E_{1/2}$, mV *vs* NHE	log $k_{cat}(O_2^{\cdot-})$	log P_{OW}
MnT-2-PyP^{+} *	−280	4.29	
MnTPP^{+} *	−270	4.83	
MnTBAP^{3-} *	−194	3.16	
$MnBr_8TM\text{-}3\text{-}PyP^{4+}$	+468	>8.85	
$MnTCl_5TE\text{-}2\text{-}PyP^{4+}$	+560	8.41	
MnTM-2-PyP^{5+}	+220	7.79	−8.16[d]
MnTE-2-PyP^{5+}	+228	7.76 (cyt *c*), 7.73 (p.r.)	−7.79[d]
MnTnHex-2-PyP^{5+}	+314	7.48	−3.84[e]
MnTnOct-2-PyP^{5+}	+367	7.71	−2.32[e]
MnTM-4-PyP^{4+}*	+60	6.58	
MnTDE-2-ImP^{5+}*	+346	7.83	
FeTE-2-PyP(OH)$^{4+}$*	+215	8.00	
MnSalen, EUK-8	−130[a]	5.78	
MnSalen EUK-189	~−130[a]	5.78 (0.37 (IC_{50} ~l μM, NBT assay) [88]	−0.9 [88]
MnSalen, EUK-134	~−130[a]	5.78	
MnSalen, EUK-207	~−130[a]	0.48 (IC_{50} ~l μM, NBT assay) [88]	−1.41 [88]
$MitoQ_{10}$ CoQ_{10}	−105 (MitoQ/$UQH^{\cdot}$), water −427 (UQ/$UQH^{\cdot}$), aprotic solvents	8.30, $k_{ox}(O_2^{\cdot-})$	3.44 (37°C, n-octanol/PBS [89] 20.26
Nitroxide, Tempone [b]	+918 [90]		
Nitroxide,[b] MitoCarboxyproxyl*[b]	+792 (3-carboxyproxyl)		
Nitroxide, Mito-Tempol*[b]	+810 (Tempol)	5.53 (Tempol)	
$MnMImP_3P^{2+}$ [72]		6.92	4.78
Mn^{2+}	+850[c]	6.11 (cyt *c*), 6.28 (p.r.)	0
SOD enzymes	~+300	8.84–9.30	

[a] estimate; no effect of structural modifications on the SOD-like activity of compounds of EUK series has been observed. Thus, we can safely estimate that all 4 listed analogues have similar $E_{1/2}$ and k_{cat};

[b] the one-electron reduction potentials refer to $RNO^{+}/RNO^{\cdot}$ redox couple which is involved in the reaction of nitroxides with superoxide and peroxynitrie [46];

[c] oxidation potential only, Mn^{III}/Mn^{II} redox couple is irreversible;

[d] calculated according to the equation log P_{OW} = 12.207 × R_f − 8.521;

[e] determined experimentally using n-butanol and water biphasic system and converted to log P_{OW} according to the equation lop P_{OW} = 1.55 × P_{BW} − 0.54 [91, 92]. When references are not indicated, the data are taken from refs [44–46].